Ubiquinone Pair in the Q_o Site Central to the Primary Energy Conversion Reactions of Cytochrome bc_1 Complex†

Huangen Ding,‡,|| Christopher C. Moser,‡ Dan E. Robertson,‡ Mariko K. Tokito,§ Fevzi Daldal,‡,§ and P. Leslie Dutton*,‡

The Johnson Research Foundation, Department of Biochemistry and Biophysics and Department of Biology, Plant Science Institute, University of Pennsylvania, Philadelphia, Pennsylvania 19104

Received April 10, 1995; Revised Manuscript Received September 7, 1995⊗

ABSTRACT: The mechanistic heart of the ubihydroquinone−cytochrome *c* oxidoreductase (cyt bc_1 complex) is the catalytic oxidation of ubihydroquinone (QH_2) at the Q_o site. QH_2 oxidation is initiated by ferri-cyt *c*, mediated by the cyt c_1 and [2Fe-2S] cluster of the cytochrome bc_1 complex. QH_2 oxidation in turn drives transmembrane electronic charge separation through two *b*-type hemes to another ubiquinone (Q) at the Q_i site. In earlier studies, residues F144 and G158 of the *b*-heme containing polypeptide of the *Rhodobacter capsulatus* cyt bc_1 complex were shown to be influential in Q_o site function. In the present study, F144 and G158 have each been singly substituted by neutral residues and the dissociation constants measured for both Q and QH_2 at each of the strong and weak binding Q_o site domains (Q_{os} and Q_{ow}). Various substitutions at F144 or G158 were found to weaken the affinities for Q and QH_2 at both the Q_{os} and Q_{ow} domains variably from zero to beyond 10^3-fold. This produced a family of Q_o sites with Q_{os} and Q_{ow} domain occupancies ranging from nearly full to nearly empty at the prevailing $\sim 3 \times 10^{-2}$ M concentration of the membrane ubiquinone pool (Q_{pool}). In each mutant, the affinity of the Q_{os} domain remained typically 10−20-fold higher than that of the Q_{ow} domain, as is found for wild type, thereby indicating that the single mutations caused comparable extents of the weakening at each domain. Moreover, the substitutions were found to cause similar decreases of the affinities of both Q and QH_2 in each domain, thereby maintaining the Q/QH_2 redox midpoint potentials (E_{m7}) of the Q_o site at values similar to that of the wild type. Measurement of the yield and rate of QH_2 oxidation generated by single turnover flashes in the family of mutants suggests that the Q_{os} and Q_{ow} domains serve different roles for the catalytic process. The yield of the QH_2 oxidation correlates linearly with Q_{os} domain occupancy (QH_2 or Q), suggesting that the Q_{os} domain exchanges Q or QH_2 with the Q_{pool} at a rate which is much slower than the time scale of turnover. On the other hand, the rate constants of the first QH_2 oxidation, ranging in the mutants from 1620 to <5 s^{-1}, correlate with the K_D values of QH_2 and Q at the Q_{ow} domain in a simple kinetic model in which the Q_{ow} domain exchanges Q or QH_2 with the Q_{pool} at a rate which is much faster than the time scale of turnover as constrained by the k_{cat} (approximately 1700 s^{-1}). The second QH_2 oxidation at the Q_o site (required for completion of the catalytic turnover of the cyt bc_1 complex) proceeds maximally at 350 s^{-1} in the wild type, and the yield and rate are affected by the single substitutions at F144 and G158 in parallel to those of the first QH_2 oxidation. A plausible mechanism is presented in which the two ubiquinones of the Q_o site cooperate in the primary steps of the catalytic action of the cyt bc_1 complex. Key features of the mechanism are as follows: (1) The formation of ubisemiquinone in both the Q_{os} and Q_{ow} domains is highly unfavorable. This keeps the steady-state concentration of the reactive semiquinone to vanishingly low levels, and hence diminishes wasteful side reactions. (2) The Q_{os} and Q_{ow} domains provide a conduit for the rapid movement of semiquinone away from the oxidizing side (the [2Fe-2S] cluster, cyt c_1 and cyt c_2) to reduce the cyt b_L. This process confers the directional specificity of the reaction, and minimizes the lifetime of semiquinone and wasteful side reactions. (3) A linear arrangement of the ubiquinones in the Q_{os} and Q_{ow} domains allows the position of the cyt b_L to be at a maximum distance from the [2Fe-2S] cluster and thus stabilizes ferro-cyt b_L with respect to the wasteful back-reaction from ferro-cyt b_L to reoxidized [2Fe-2S] cluster. This strongly favors the physiologically useful electron transfer from ferro-cyt b_L to ferri-cyt b_H and the Q in the Q_i site.

The ubihydroquinone−cytochrome *c* oxidoreductase (cyt bc_1 complex)[1] is an integral membrane protein that drives the separation of charge and proton movement across the supporting membrane (Dutton, 1986; Cramer & Knaff, 1989; Prince, 1990; Trumpower, 1990). In photosynthetic bacteriasuch as *Rhodobacter capsulatus*, the reactions of the cyt

† Research support is acknowledged from Public Health Service Grants GM 27309 to P.L.D. and GM 38237 to F.D. The authors are indebted to J. Baz Jackson and Eryl Sharp for valuable discussions and critical reading of the manuscript.

* Address correspondence to this author at B501 Richards Building, Johnson Research Foundation, Department of Biochemistry and Biophysics, University of Pennsylvania, Philadelphia, PA 19104. Telephone: (215) 898-8699. Fax: (215) 573-2235. E-mail: dutton@mail.med.upenn.edu.

‡ Department of Biochemistry and Biophysics.

§ Department of Biology.

|| Present address: Laboratory of Cellular and Molecular Toxicology, Harvard School of Public Health, Boston, MA 02115.

⊗ Abstract published in *Advance ACS Abstracts,* November 1, 1995.

[1] Abbreviations: $\Delta G°$, standard Gibbs free energy; λ, reorganization energy−summed energies of structural rearrangements associated with redox cofactors, protein, and solvent coupled to electron transfer; cyt, cytochrome; cyt bc_1, ubihydroquinone−cyt c_2 oxidoreductase; cyt b_H, high potential cyt *b* of cyt bc_1; cyt b_L, low potential cyt *b* of cyt bc_1; E_h, redox potential versus the standard hydrogen electrode; E_{m7}, electrochemical midpoint potential at pH 7.0; EPR, electron paramagnetic resonance; Q, ubiquinone; QH_2, ubihydroquinone; Q_i, Q reducing site of cyt bc_1 complex; Q_o site, QH_2 oxidizing site of cyt bc_1 complex; Q_{os}, ubiquinone strongly binding domain of the Q_o site; Q_{ow}, ubiquinone weakly binding domain of the Q_o site; SQ, ubisemiquinone.

0006-2960/95/0434-15979$09.00/0

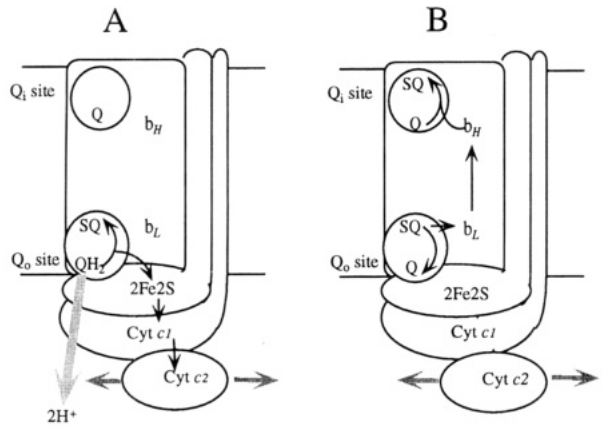

FIGURE 1: Arrangement of the redox centers in the cyt bc_1 complex. The arrangement of the redox centers ubiquinones, cyt b_L, cyt b_H, [2Fe-2S] cluster and cyt c_1 of the cyt bc_1 complex, and cyt c_2 is based on the information from biophysical, biochemical, and genetic characterizations of the protein (see text for descriptions). Part A shows the electron transfer steps from QH_2 to ferri-cyt c_2 via the [2Fe-2S] cluster and cyt c_1. Part B shows the electron transfer from the semiquinone (SQ) produced in part A to Q in the Q_i site via cyt b_L and cyt b_H. The gray arrow in part A suggests the release of two protons from the Q_o site. The arrows associated with cyt c_2 indicate its lateral motion.

bc_1 complex are driven by the redox free energy difference between ferri/ferro-cyt c_2 ($E_{m7} = 340$ mV; Prince & Dutton, 1977) and ubiquinone/ubihydroquinone (Q/QH_2) ($E_{m7} = 90$ mV; Ding et al., 1992), as traditionally presented as follows:

$$2\text{ferri-cyt } c_2 + QH_2\ (Q_{pool}) = 2\text{ferro-cyt } c_2 + Q\ (Q_{pool}) + 2H^+ \quad (1)$$
$$\Delta G^\circ = -500 \text{ meV or } -11.5 \text{ kcal/mol } QH_2 \text{ oxidized}$$

Figure 1 shows a schematic picture of the cyt bc_1 complex and the location of its redox cofactors in the membrane profile as determined in *R. capsulatus* (Robertson & Dutton, 1988) and generalized in several recent reviews (Degli Esposti et al., 1993; Brandt & Trumpower, 1994; Gray & Daldal, 1995). The cyt bc_1 complex protein is made up of three subunits that accommodate one [2Fe-2S] cluster, one cyt c_1, and two cyts b [designated b_H and b_L, according to their relatively high ($E_{m7} = 50$ mV) and low ($E_{m7} = -90$ mV) redox midpoint potentials (Dutton et al., 1970; Dutton & Jackson, 1972; Petty & Dutton, 1976; Meinhardt & Crofts, 1983; Robertson & Dutton, 1988; Robertson et al., 1993)]. The cyt bc_1 complex also accommodates two essential and distinct ubiquinone binding sites for the interaction with the ubiquinone pool (Q_{pool}) in the membrane. The sites, called the Q_o and Q_i sites, catalyze QH_2 oxidation and Q reduction, respectively, and choreograph the exchange of protons with the aqueous phases on either side of the membrane (Mitchell, 1976; Dutton, 1986; Robertson & Dutton, 1988; Cramer & Knaff, 1989; Prince, 1990; Trumpower, 1990; Gennis et al., 1993; Brandt & Trumpower, 1994; Gray & Daldal, 1995).

The overall reaction shown by eq 1 involves the sum of two separate QH_2 to Q oxidations at the Q_o site and the reduction of one Q to QH_2 at the Q_i site. The Q_o site exchanges Q for QH_2 drawn from the Q_{pool} with a ΔG° value near zero (Ding et al., 1992). The first QH_2 oxidized at the Q_o site leads to the reduction (via the [2Fe2S] cluster and cyt c_1) of one ferri-cyt c_2 and the reduction (via cyt b_L and cyt b_H) of a Q at the Q_i site to a semiquinone (SQ). The E_{m7} value of SQ/Q in the Q_i site is 30 mV (Robertson et al., 1984). This is shown by

$$\text{ferri-cyt } c_2 + QH_2\ (Q_o) + Q\ (Q_i) = \text{ferro-cyt } c_2 + Q\ (Q_o) + SQ\ (Q_i) + 2H^+ \quad (2A)$$
$$\Delta G^\circ = -190 \text{ meV or } -4.38 \text{ kcal/mol}$$

The product Q at the Q_o site returns to the Q_{pool} but the semiquinone at the Q_i site is thought to stay in place like that well established for the Q_B site of the photosynthetic reaction center (Wraight, 1979). A second QH_2 oxidized at the Q_o site leads to the reduction of another ferri-cyt c_2 and the reduction of the SQ at the Q_i site to QH_2. The E_{m7} of the QH_2/SQ in the Q_i site is 270 mV (Robertson et al., 1984) as shown in eq 2B. The catalytic cycle is completed when the QH_2 produced in the Q_i site exchanges with Q from the Q_{pool}; this has a ΔG° penalty of +120 meV (Ding et al., 1992):

$$\text{ferri-cyt } c_2 + QH_2\ (Q_o) + SQ\ (Q_i) = \text{ferro-cyt } c_2 + Q\ (Q_o) + QH_2\ (Q_i) \quad (2B)$$
$$\Delta G^\circ = -430 \text{ meV or } -9.92 \text{ kcal/mol}$$

The driving force for these reactions comes in part from the free energy in the electron transfer between the cyt c_2 and the [2Fe-2S] cluster (about −70 meV or −1.6 kcal/mol) but predominantly from the electron transfer from cyt b_L to cyt b_H and then to the Q in the Q_i site (−120 meV or −2.76 kcal/mol for the first and −360 meV or −8.28 kcal/mol for the second QH_2 oxidized). This free energy is harnessed for the generation of the principal energetic product of the cyt bc_1 complex, a transmembrane potential.

In contrast to these large free energy reactions, the steps which are primary to this energy conversion, catalyzed in the Q_o site, display an overall free energy that is surprisingly close to zero (Ding et al., 1992) as shown in eq 3:

$$[2Fe2S]^{ox} + QH_2\ (Q_{pool}) + \text{ferri-cyt } b_L = [2Fe2S]^{red} + Q(Q_{pool}) + \text{ferro-cyt } b_L \quad (3)$$
$$\Delta G^\circ = -18 \text{ meV or } -0.41 \text{ kcal/mol}$$

Very little is known in any species about the Q_o site catalyzed primary events of energy conversion in the cyt bc_1 complex. A working model of the Q_o site in the cyt bc_1 complex of photosynthetic bacteria has been drawn from the ubiquinone extraction−reconstitution studies of Ding et al. (1992). These studies showed that there are two ubiquinone binding domains in the Q_o site. One of the domains was determined to have a strong affinity and the other a weak affinity for Q/QH_2, and accordingly they were designated Q_{os} and Q_{ow} domains of the Q_o site, respectively. Functionally, it was suggested that the two domains were present to accommodate the requirement, described in eqs 2A and 2B, for two QH_2 oxidized at the Q_o site to complete the full catalytic turnover. The ubiquinones of both domains were considered by Ding et al. (1992) to be in rapid exchange with the Q_{pool} to initiate new turnovers. The present work explores this idea further with a view to obtain a better definition of the function of quinones in the two domains

and to describe the individual steps of the primary electron transfer sequences.

We examine the effects of substituting two amino acid residues of the cyt *b* polypeptide that have previously been shown to influence the activity of QH_2 oxidation in the Q_o site. One is phenylalanine at position 144 (F144) recognized in an inhibitor resistance study (Robertson et al., 1990), and the other one is glycine at position 158 (G158) originally studied as the spontaneous mutant R126 (Zannoni & Marrs, 1981; Robertson et al., 1986) and later identified as G158D (Daldal et al., 1989). The results demonstrate that the principal effect in the majority of a wide range of simple neutral substitutions at the F144 and G158 positions is the parallel weakening of the affinity of QH_2 and Q for both the Q_o site domains. In this family of site-directed mutants, correlation of the affinity data with flash-induced yields and rates of QH_2 oxidation strongly suggests that the Q/QH_2 of the Q_{os} domain remains in the Q_o site throughout the catalytic cycle while that of the Q_{ow} domain is in rapid exchange with the Q_{pool}. The family of mutants provides a thermodynamic view of the ubiquinones of the two Q_{os} and Q_{ow} domains cooperating in the primary catalytic events in the cyt bc_1 complex.

MATERIALS AND METHODS

Cells and Routine Analyses of Chromatophore Preparations

The single site-directed mutants used in this work were constructed at F144 and G158 in the cyt *b* polypeptide of the cyt bc_1 complex from *R. capsulatus* as described in Atta-Asafo-Adjei and Daldal (1991). The mutants chosen for the study were simple neutral aliphatic and aromatic residue substitutions; for others, see the accompanying paper (Ding et al. 1995). Mutant strains of the F144 series were grown anaerobically under photosynthetic conditions; under such conditions the growth rates were perfectly adequate for the production of experimental material. In the G158 series, only G158A, S, and P could be grown photosynthetically, and therefore all organisms in this group were grown microaerobically [see Atta-Asafo-Adjei and Daldal (1991) and Tokito and Daldal (1993)]. Cells were harvested in late log phase, and chromatophore membranes were prepared as described in Robertson et al. (1986).

Most redox reactants in the chromatophore membranes were assayed using a Johnson Research Foundation type (University of Pennsylvania) dual-wavelength spectrophotometer equipped with an anaerobic cuvette under an argon atmosphere. Xenon flash activation (half-width 8 μs) was delivered to the cuvette from underneath. The anaerobic cuvettes and accompanying redox potentiometric poising for kinetic work and EPR analysis was as described in Dutton (1978) [see also Ding et al. (1992)]. In all work the chromatophores were suspended in 100 mM KCl, 50 mM MOPS buffer, pH 7.0. The reaction center concentration in chromatophore suspensions was assayed by flash activated oxidation of the bacteriochlorophyll dimer ($BChl_2^+$) measured at 605−540 nm (Dutton et al., 1975). The cyt bc_1 complex concentration was commonly measured by flash activated oxidation or reduction of its redox components (van den Berg et al., 1979); in particular, cyt b_H was measured at 561−569 nm and cyt $c_1 + c_2 + c_y$ was measured at 550−540 nm. Throughout this paper, cyt $c_1 + c_2 + c_y$ is designated simply as cyt *c*.

The apparent average concentration of the reaction center within the chromatophore membrane is calculated to be 1.2 mM, based on the density of reaction centers in chromatophore membranes as determined by Packham et al. (1978) and modified by Dutton (1986). After a single flash, the ratio of the rapidly acting cyt bc_1 complex to reaction center in the chromatophores of the various mutants was routinely found to be close to 0.5 yielding an average membrane concentration of cyt bc_1 complex of 0.6 mM. The total ubiquinone content of chromatophore membranes was measured by acetone−methanol extraction after Kröger and Klingenberg (1973) as described in Ding et al. (1992). A ratio of 25 ± 5 ubiquinone molecules per reaction center was routinely found in the wild type strain, and similar values were established in two selected mutants, F144I, and F144L (see Results). Approximately 80% of the ubiquinone found in chromatophore membrane is a homogenous pool (Q_{pool}) (Takamiya & Dutton, 1979; Ding et al., 1992). We estimate, taking the thickness of the chromatophore membrane profile available for the ubiquinone-10 hydrophobic tail and the relatively polar headgroup to be approximately 40 Å, that the apparent average concentration of ubiquinone of the homogeneous pool in chromatophores is 30 ± 6 mM. The uncertainties in these estimates are well recognized, but we believe that the use of a practical concentration rather than a reactant ratio facilitates presentation and understanding of the studies both conceptually and analytically without significantly altering the conclusions drawn. A similar line of approach has been made earlier (Crofts & Wang, 1989).

Determination of the Q_o site Occupancy by Q or QH_2 by EPR Spectroscopy

Determination of Q_o site occupancy makes empirical use of the EPR spectral line shape of the reduced [2Fe-2S] cluster to determine the Q_o site occupancy by Q or QH_2 in the cyt bc_1 complex (Ding et al., 1992; Robertson et al., 1993). All EPR spectra were taken with the chromatophore suspension poised at a redox potential of less than 230 mV to establish the [2Fe-2S] cluster in the reduced paramagnetic form. Further to this, the Q_{pool} was either essentially oxidized (200−230 mV) or reduced (−20 to 0 mV) so that the Q_{pool} species available to occupy the Q_o site was clearly either Q or QH_2. The [2Fe-2S] cluster EPR spectra were taken on a Varian E-109 X-band EPR spectrometer equipped with flowing helium cryostat (Air Products LTD 3-110). Routine instrumental conditions were as follows: field set, 3600 G; scan range, 1000 G; scan rate, 250 G/min; time constant, 0.25 s; modulation frequency, 100 kHz; modulation amplitude, 12.5 G; microwave frequency, 9.32 GHz; microwave power, 2.0 mW; temperature, 20 K.

Occupancy by Q. The EPR spectra of the reduced [2Fe2S] cluster of wild type *R. capsulatus*, obtained with different levels of Q occupancy in the Q_o site, are shown in Figure 2A. The spectra describe (a) a g_x band at 1.800 when both the Q_{ow} and Q_{os} domains in the Q_o site are occupied by Q, (b) a broadened g_x band at 1.783 when the Q_{os} domain is occupied by Q and the associated Q_{ow} domain is empty, and (d) a considerably broadened g_x band at 1.765 when the Q_{os} and Q_{ow} domains are both empty of Q. These three spectra, recorded under conditions which are as close as is experi-

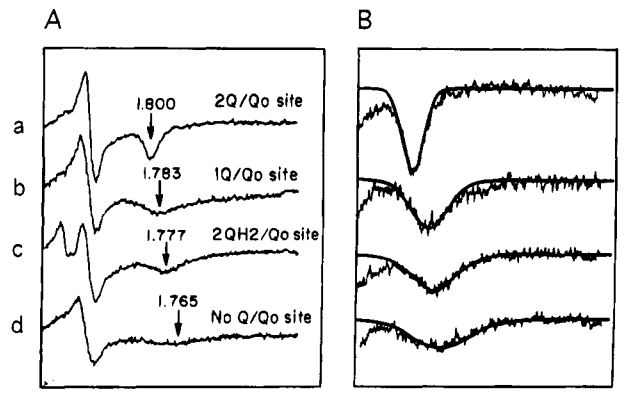

FIGURE 2: [2Fe-2S] cluster EPR spectra of the *R. capsulatus* cyt bc_1 complex with different Q_o site occupancy. Spectra were obtained from chromatophores suspended in 100 mM KCl and 50 mM MOPS, pH 7.0, containing 15 μM cyt bc_1 complex. The redox potential was adjusted to 200 ± 10 mV (for Q binding) or 0 ± 10 mV (for QH_2 binding). Part A shows EPR spectra of the [2Fe-2S] cluster with different Q_o site occupancies: (a) both Q_{os} and Q_{ow} domains are occupied ($2Q/Q_o$ site), (b) Q is present in the Q_{os} domain only ($1Q/Q_o$ site), (c) one or two QH_2 are present in the Q_{os} and Q_{ow} domains [1 or $2QH_2/Q$ site; there is no apparent difference in the [2Fe2S] EPR lineshape when the Q_o site binds one or two QH_2 [see Ding et al. (1992)]], and (d) no Q or QH_2 is present in either domain (no Q/Q_o site). Part B details the g_x band of the spectra in part A. The solid line drawn through each g_x band is a Gaussian component fitted with a nonlinear curve fit software (Jandel Scientific Co.).

mentally possible for the achievement of single-species line shapes, provided archetypal fits through the three g_x bands as shown in Figure 2B. We note that while fits can be obtained to the entire spectrum for each state (Robertson et al., 1993), it was established over many determinations that a fit to the g_x band alone was sufficient to quantitate occupancy to a level suitable for our present purposes. Deconvolution of the g_x band of the [2Fe-2S] cluster EPR spectra of the mutants into the three archetypal components was performed using nonlinear curve-fitting software (Jandel Scientific Co.). The widths and the reasonably well-resolved positions of the g_x band archetypes yielded near unique fits. The measured fractional occupancy of the Q_{os} and Q_{ow} domains in the various batches of cells of wild type or mutants was reproducible within a 5% standard deviation.

Occupancy by QH_2. The EPR spectrum of the [2Fe-2S] cluster when QH_2 is present in the Q_o site is characterized by a g_x band at 1.777 as shown in Figure 2A (c). This is also evident in other systems (Siedow et al., 1978; Matsuura et al., 1983; de Vries et al., 1982, 1986). However, in the analysis of the QH_2 occupancy, there is no clear discrimination in the [2Fe-2S] cluster EPR spectra between occupancy of the Q_{os} domain alone and occupancy of both the Q_{os} and Q_{ow} domains (Ding et al., 1992). Thus, the change in the g_x position from 1.777 to 1.765 follows the transition from the doubly (Q_{os} and Q_{ow}) or the singly (Q_{os}) occupied state, to the situation in which the Q_o site is unoccupied. This means that this assay only gives information about the QH_2 occupancy of the Q_{os} domain and does not report on whether or not the associated Q_{ow} domain is occupied. [We note here that in the work of Ding et al. (1992) this point was not well appreciated. In the reported redox titrations, the transition from g_x 1.800 to 1.777 was tentatively identified with the reduction of Q to QH_2 in the Q_{ow} domain. Hence, the reported redox midpoint potentials (E_{m7}) for Q/QH_2 in the Q_{ow} domain more correctly represented the reduction of

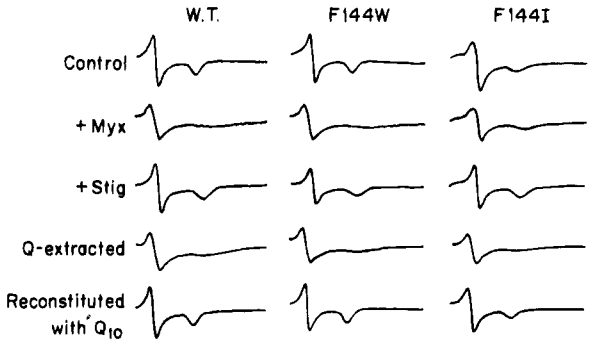

FIGURE 3: EPR spectra of [2Fe-2S] cluster of selected mutants after addition of Q_o site inhibitors or after Q extraction and reconstitution. All EPR spectra of the [2Fe-2S] cluster were taken in chromatophores suspended in 100 mM KCl and 50 mM MOPS, pH 7 containing approximately 15 μM cyt bc_1 complex. The redox potential of the suspension was adjusted to 200 ± 10 mV at pH 7.0. The final concentration of the Q_o site inhibitors, stigmatellin and myxothiazol, was 75 μM.

Q to QH_2 in the Q_{os} domain when the Q_{ow} domain was occupied.] The reproducibility of the determination of QH_2 occupancy of the Q_{os} domain (with the Q_{ow} domain either occupied or unoccupied) from one batch preparation to another was found to be within 10% experimental error.

Determination of the Dissociation Constants from the Q_o Site Occupancies. Dissociation constants (K_D values) for Q or QH_2 in the Q_{os} domain and Q in the Q_{ow} domain of the Q_o site were calculated from the Q_{os} and Q_{ow} domain occupancies as shown for Q in eq 4.

$$K_{DQ} = \frac{[Q_o][Q]}{[Q_oQ]} \quad (4)$$

In eq 4, [Q] (or alternatively $[QH_2]$) represents the Q_{pool} concentration of Q (or QH_2) in the chromatophore membrane (30 ± 6 mM) as described above; $[Q_o]$ represents the concentration of empty Q_{os} or Q_{ow} domain and $[Q_oQ]$ is the concentration of the Q_{os} or Q_{ow} domain occupied with Q (or QH_2). The Q_o site concentration in the chromatophore membrane is given by that of the cyt bc_1 complex which is 0.6 mM based on the calculations discussed above.

Preliminary EPR Analysis of the Mutants

The EPR line shapes of the [2Fe-2S] cluster of each mutant were initially inspected to establish suitability for quantitative analysis of the Q_o site occupancy. Spectra were examined in the presence of the Q_o site-specific inhibitors myxothiazol and stigmatellin, which are well-known to establish EPR spectra of the [2Fe-2S] cluster that are characteristic of their Q_o site occupancy in cyt bc_1 complexes from a variety of sources (de Vries et al., 1982; von Jagow & Ohnishi, 1985; Tsai et al., 1985; Ohnishi et al., 1988; Ding et al., 1992; Robertson et al., 1993). They were also examined when the Q_{pool} was poised in either the Q or QH_2 states and, in representative cases, after extraction and reconstitution with various levels of ubiquinone in chromatophore membranes.

Figure 3 shows some representative spectra of the mutants and the wild type in the presence of inhibitors or when the Q_{pool} was completely extracted. In the presence of excess Q_o site-specific inhibitors, stigmatellin or myxothiazol, all mutants displayed [2Fe-2S] cluster EPR line shapes identical to those that are well established for the wild type when these

inhibitors are bound to the Q_o site (data not shown). When representative mutants (F144W, F144I, F144S) were fully extracted of their Q_{pool} complements, they displayed the same broad EPR spectrum as that in the wild type with an empty Q_o site, as detailed in Figure 2d. Furthermore, as indicated by the mutants F144W and F144I, reconstitution at various levels with ubiquinone-10 were always found to be firm composites of the archetypal line shapes. In no case was there evidence that the mutations induced disturbances to the inhibitor−Q_o site−[2Fe-2S] cluster interaction or themselves directly caused any alterations of the [2Fe-2S] cluster EPR spectra.

Finally, while making empirical use of the [2Fe-2S] cluster EPR spectra to determine the Q_o site occupancy, we have recognized (Ding et al., 1992) that the presence of certain solvents diminishes or abolishes the sensitivity of the [2Fe-2S] cluster EPR line shape as an assay of the Q_o site occupancy by Q or QH_2. Such solvents include the short chain alcohols and polyols that are in common use as solvents for solute addition or for storage of the chromatophore membranes. In contrast, dimethyl sulfoxide (DMSO) at concentrations well above that used in the experiments reported here has proven to have little or no effect on the [2Fe-2S] cluster EPR spectra. Because of this, DMSO was used throughout as the solvent of choice for the redox mediators and inhibitors.

Electron Transfer Kinetics in the Q_o Site of the Cyt bc_1 Complex

For all kinetic measurements described in this report, valinomycin (2 μM) was present to eliminate any energetic feedback effects on the reaction yield or rate from the generation of membrane electrochemical gradients [see Robertson and Dutton (1988)].

QH_2 Oxidation Rates and Yields. The rate of the first QH_2 oxidation was determined from the course of flash activated reduction of cyt b_H in the presence of the Q_i site inhibitor antimycin [see Robertson et al. (1990)]. For rates measured with the Q_{pool} reduced and hence with only QH_2 at the Q_o site prior to activation, the chromatophores were poised at redox potentials of 40 ± 10 mV. This potential ensures that the Q_{pool} comprises >90% QH_2 but does, in fact, also establish the cyt b_H 40−70% reduced prior to activation. This means that the flash activated amplitude of cyt b_H reduction is correspondingly diminished, but fortunately not prohibitively. For rates measured with the Q_{pool} virtually fully oxidized and hence with only Q at the Q_o site prior to activation, the redox potential was poised at 200−230 mV. The kinetic traces were fit to a single-exponential component plus a constant using a Q-Basic program.

The rate of the second QH_2 oxidation in the Q_o site was determined from the rate of the observable flash-oxidized cyt *c* re-reduction or the flash-reduced cyt b_H re-oxidation measured in the absence of the Q_i site inhibitor antimycin (Robertson et al., 1990). For the rates measured with the Q_{pool} comprising only QH_2 prior to activation, the kinetics and analysis were as described above for the first QH_2 oxidized. In contrast, kinetic analysis of the second QH_2 oxidation measured with the Q_{pool} comprising only Q before activation was not done. This is because under these conditions the substrate QH_2 must be generated by the Q_B site of the flash activated reaction centers. As such QH_2 is produced in limiting quantities (i.e., ~1.0 QH_2 per cyt bc_1 complex) and since two QH_2 oxidation are needed to complete the full turnover of each cyt bc_1 complex, the kinetics of the "second QH_2" oxidized are expected to be complex [see Matsuura et al. (1981)].

Reaction yields of the QH_2 oxidation following single flash activation were obtained as a matter of course during the rate determinations and found to vary in the mutants. Hence, yields were obtained for the first and second QH_2 oxidized when the Q_{pool} was all Q or QH_2 as described above. However, yields measured when the Q_{pool} was >90% QH_2 (redox potential 40 ± 10 mV), and which also established the cyt b_H itself 40−70% reduced, was sensitive to small variations in the values of poised redox potential. As a backup therefore, the yield was additionally measured at approximately 100 mV, a redox potential that poises the cyt b_H 90% oxidized where it is relatively insensitive to variation with redox potential but which is low enough to establish a Q_{pool} that approached about 30% reduced QH_2.

Estimations of Q_o Site Dissociation Constants for QH_2 from Rates and Yields. A simple pre-steady-state kinetic model was considered in this work to serve as an exploratory means to obtain K_D values for the QH_2 (substrate) at the Q_{os} and Q_{ow} domains of the Q_o site. A foothold into the kinetic analysis was based on the previous finding (Ding et al., 1992), and verified here, that the wild type Q_o site operates with both the Q_{os} and Q_{ow} domains essentially fully occupied. Thus, when the Q_{pool} is fully reduced in wild-type chromatophores, the observed rate (k_{obs}) of QH_2 oxidation in the catalytic cycle is expected to approach the value of k_{cat} for the reaction and go to completion, approaching 100% yield.

For the case where QH_2 is exchanging between the Q_o site and the Q_{pool} at a rate faster than k_{cat}, a K_D value can be obtained from

$$K_{DQH_2} = \frac{k_{cat}[QH_2]}{k_{obs}} - [QH_2] \quad (5)$$

In eq 5 k_{cat} is the catalytic rate of the QH_2 oxidation and k_{obs} is the flash activated QH_2 oxidation rate in the absence of product Q. The concentration of [QH_2] of the membrane pool was taken to be 30 ± 6 mM as discussed above under *Cells and Routine Analyses of Chromatophore Proteins.*

For the case where the QH_2 is exchanging between the Q_o site and the Q_{pool} at a rate much slower than the k_{cat} value, the K_D value can be obtained from single flash activated reaction yields. Reaction yield of the first and second QH_2 oxidized relative to the wild type provided fractional occupancies of the site at the time of activation and during the entire sequence of catalysis; K_D values were obtained from the fraction of occupanices applied to eq 4. This has been done before for similar work on the Q_A site of the photosynthetic reaction center (Gunner et al., 1985; Gunner & Dutton, 1989; Giangiacomo & Dutton, 1989).

Redox Midpoint Potentials of the Q_o Site Q/QH_2 Couples

Midpoint potentials at pH 7 (E_{m7}) for the Q_o site Q/QH_2 couples were determined in three ways. In the first method the E_{m7} values were calculated from the K_D values of Q and QH_2 in the sites according to

$$\log[(K_{DQH_2})/(K_{DQ})] = (E_{m7(Q_{pool})} - E_{m7(Q_o)})/30 \quad (6)$$

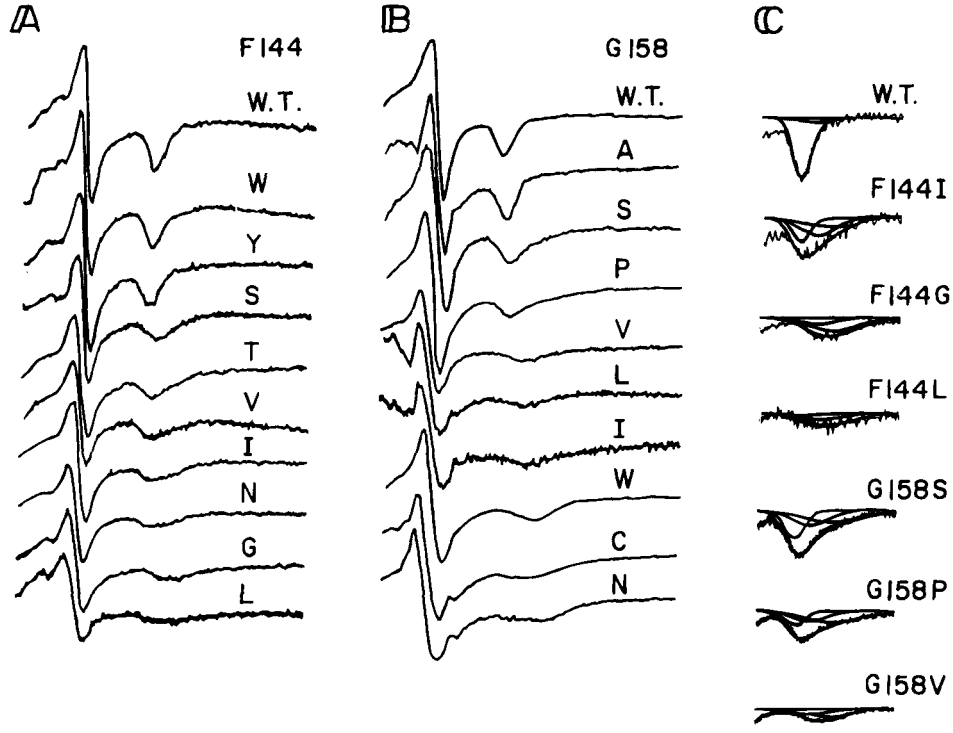

FIGURE 4: Q_o site Q occupancy of the mutants F144 and G158. The concentrations and conditions are as described as in the legend to Figure 1. Parts A and B show EPR spectra of the [2Fe-2S] cluster of wild type and mutants at F144 and G158, respectively. Part C shows the representative deconvolutions of the selected g_x band from parts A and B. Three g_x components (1.800, 1.783, and 1.765) as shown in Figure 2B were fitted to the g_x bands of various mutants.

Equation 6 applies to the experimental temperature of 295 K; the E_{m7} value of the Q/QH_2 couple in the Q_{pool} of *R. capsulatus* is 90 ± 10 mV (Ding et al., 1992).

The second method involved direct redox potentiometric titration of the g_x band of the [2Fe2S] cluster EPR spectrum over the redox potential (E_h) range of 300 to −50 mV as referred to above in *Cells and Routine Analyses of Chromatophore Proteins*; and for earlier work see Ding et al. (1992). The change of the g_x position as a function of E_h follows the course of reduction of ubiquinone associated with the Q_{os} domain in the Q_o site domains as is discussed above in *Determination of the Q_o Site Occupancy by Q or QH_2 by EPR Spectroscopy.*

In the third method, apparent E_{m7} values were obtained from redox titration (300 to 40 mV) of the rate of cyt *b* reduction in the presence of antimycin (first QH_2 oxidized) and the rate of cyt *c* re-reduction in the absence of the Q_i site inhibitor (second QH_2 oxidized) as described above in *Electron Transfer Kinetics in the Q_o Site of the Cyt bc_1 Complex.*

Chemicals

These were as described in Ding et al. (1992).

RESULTS

The Equilibrium Interaction of Q/QH_2 with the Q_o site of the F144 and G158

Mutants Determined by the EPR Method: (a) [2Fe-2S] Cluster EPR Spectra (i) Spectra with Q Present. Figure 4 shows the [2Fe-2S] cluster EPR spectra of F144 and G158 substituted Q_o sites poised so that the Q_{pool} was entirely comprised of Q. The spectra are arranged roughly in order of decreasing Q occupancy of the Q_o site as indicated by comparison with spectra a, b, and d of Figure 2.

Figure 4A shows that when residue F144 is substituted with other aromatic residues, tyrosine (Y) and tryptophan (W), the resulting mutants share the same spectral characteristic as the wild type with g_x at 1.800, g_y at 1.890, and g_z at 2.020. These spectra indicate that the Q_{os} and Q_{ow} domains in the Q_o site remain nearly fully occupied. In contrast, the spectra of F144S, T, V, I, N, and G yield increasingly broadened spectra with the g_x band moving toward and beyond 1.783 until, with F144L, the g_x band is shifted to 1.765. This indicates that, upon replacement of phenylalanine 144 with these neutral nonaromatic residues, the Q_{os} and Q_{ow} domains both suffer major losses in affinity for Q and become partially or severely depleted at the prevailing native Q_{pool} concentration of chromatophore membranes.

Figure 4B shows that the substitutions of G158 display a similar set of variations in the [2Fe-2S] cluster EPR spectra. G158A yields a g_x band indicative of the Q_{os} and Q_{ow} domains that remain nearly fully occupied with Q. The g_x bands of the G158S and G158P suggest that the affinities of the Q_{os} and Q_{ow} domains are lowered, thus leading to partial occupancy. The other substitutions examined (G158V, L, I, W, C, and N) displayed a g_x at 1.765 suggesting that both Q_{os} and Q_{ow} domains are almost empty in these mutants. It appears that the affinities of the Q at the Q_{os} and Q_{ow} domains in the Q_o site are more sensitive to changes at position G158 than at F144.

Figure 4C shows examples of the quantitative analysis of the [2Fe-2S] cluster EPR spectra from selected F144 and G158 substitutions and the wild type. In these and all other mutants, fits to the observed g_x band region could be accommodated with no significant residuals by combinations of archetypal g_x bands a, b, and d as shown in Figure 2B.

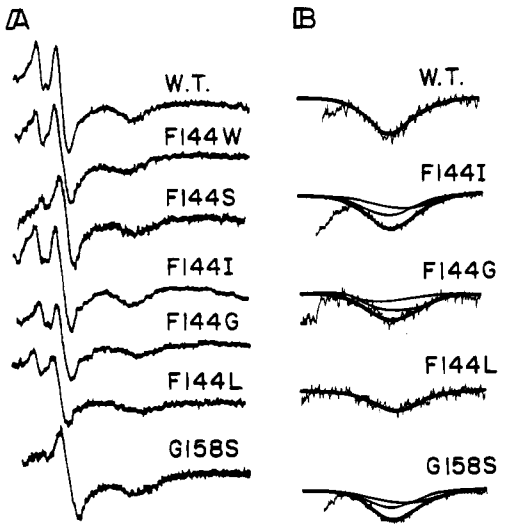

FIGURE 5: Q_o site QH_2 occupancy of the mutants F144 and G158. EPR spectra of the [2Fe-2S] cluster of the wild type and the representative mutants of F144 and G158 are shown when the Q_{pool} is reduced. Samples were prepared as in Figure 4 except the redox potential was adjusted to 0 ± 10 mV(pH 7.0) so that the Q_{pool} was comprised of only QH_2. Part B shows representative deconvolutions of the g_x band from part A with two Gaussian components (g_x at 1.777 and 1.765) as shown in Figure 2B.

(ii) Spectra with QH_2 Present. Figure 5A shows [2Fe-2S] cluster EPR spectra of some F144 and G158 substituted Q_o sites poised so that the Q_{pool} was entirely comprised of QH_2. Figure 5B shows examples of the quantitative analysis of [2Fe-2S] cluster EPR spectra using fits from the archetypal g_x bands c and d of Figure 2B. In general, the occupancy of QH_2 in the Q_{os} domain of each mutant was similar to that found for Q.

(b) Q and QH_2 Occupancies and Dissociation Constants in the Q_o Site. Table 1 columns A–E list the resolved archetypal spectral components of the EPR spectra of the wild type and mutants, and columns F–J list the calculated fractional occupancies of Q and QH_2 in the Q_{os} and Q_{ow} domains. Columns K and L present the K_D values for Q and QH_2 in the Q_{os} domains and column M presents the K_D values for Q in the Q_{ow} domain calculated according to eq 4. It is evident that substitutions at F144 and G158 alter the K_D values for both Q and QH_2 in the Q_{os} domain and Q in the Q_{ow} domain that span well over three orders of magnitude. Despite this enormous range of effect between the different mutants, the variance of the individual substitution effects on the three K_D values for a particular mutant did not extend beyond a 5-fold range in each mutant.

(c) General Correlation of the Dissociation Constants from the Q_o Site with Cyt bc_1 Complex Activity. Table 1, column N, lists the relative cyt bc_1 complex activities of the mutants. It is evident that as the affinity of the Q_o site for Q or QH_2 becomes progressively weakened, the cyt bc_1 complex displays decreased activity.

Yields and Rates of QH_2 Oxidation in Selected F144 and G158 Mutants

Examples of the key flash activated QH_2 reaction kinetics of nine mutants selected for detailed study from the neutral substitutions in positions F144 and G158 are shown in Figure 6. This figure shows the time course of the first QH_2 oxidation (cyt b_H reduction) and second QH_2 oxidation (cyt *c* re-reduction) at the Q_o site measured when the Q_{pool} is nearly fully reduced, about half oxidized and fully oxidized. The striking result evident in Figure 6 is the finding that the QH_2 oxidation reaction varies dramatically in the mutants, not just in reaction rate, but also in reaction yield. The yields and rates of the QH_2 oxidation after single flash activation are listed in Table 2.

(a) Relative Yields, (i) Measurement. Columns A, B, and C of Table 2 list the reaction yield relative to the wild type measured under various conditions in the different mutants. Columns A and B demonstrate that the relative yield in any one mutant does not vary, despite the 5–12-fold difference in the rates of QH_2 oxidation that are encountered when the Q_{pool} is all QH_2 or all Q prior to flash activation (columns E and F). Moreover, the yield does not vary between the first and second QH_2 oxidized (columns A, B, and C). In general, although the relative yield diminishes from unity to near zero as the rate slows, it is clear that the loss of yield is not the result of a slowed forward QH_2 oxidation rate that fails to compete with some characteristic decay rate of the activated state at the Q_o site. These data strongly suggest that the occupancy of one of the domains of the Q_o site by Q or QH_2 is a prerequisite for catalysis and that the exchange rate between this domain and the Q_{pool} must be slow compared to the lifetime of the flash activated state and catalytic turnover.

(ii) Correlation of the Relative Yields of QH_2 Oxidation to the Occupancy of the Q_{os} and Q_{ow} Domains. Figure 7 explores the relationship between the relative yield of QH_2 oxidation and the occupancies of the Q_{os} and Q_{ow} domains established by EPR for the various mutants. Figure 7A reveals a linear relationship between the relative yields of first and second QH_2 oxidation reactions and the EPR determined occupancy of the Q_{os} domain by either QH_2 or Q at the time of activation. Figure 7B shows that the relationship between relative yield and the Q_{ow} domain occupancy is strongly hyperbolic and, in comparison with assignment to the Q_{os} domain occupancy, is far more difficult to explain. Thus, the occupancy of the Q_{os} domain appears to be the most likely possibility for explaining the variance in yield. This identification suggests that the QH_2 in the Q_{os} domain is in slow exchange with the Q_{pool}. Moreover, it is evident that occupancy of this domain is mandatory for initiation and completion of Q_o site catalytic turnover of the cyt bc_1 complex.

(iii) K_D Values for the Q_{os} Domain from the Relative Yields. The most straightforward determination of K_D values from the relative yields (see *Estimations of Q_o Site Dissociation Constants for QH_2 from Rates and Yields* under Materials and Methods) is for the first QH_2 oxidation when there is only QH_2 present at the time of flash activation (Table 2, column A). Figure 8A presents these data graphically, and Table 2, column D, lists the calculated K_{DQH_2} (yield) values.

Table 3 allows comparison of the K_D values determined by EPR with those determined from reaction kinetics. The table shows that the K_{DQH_2} (yield) values are remarkably similar to the independently determined K_{DQH_2} (EPR) values of the Q_{os} domain, providing support for the idea that occupancy of the Q_{os} domain controls the reaction yield. It is concluded that the equilibrium occupancy of the Q_{os} domain, whether monitored directly by EPR or indirectly from the flash activated QH_2 oxidation relative yield,

Table 1: Q_o Site Occupancy in the Mutants with Substitutions in F144 and G158[a]

	population of g_x transitions (%)					Q_{os} and Q_{ow} occupancies					K_D[b] (mM)			
	for Q			for QH_2		for Q			for QH_2		Q_{os}		Q_{ow}	
	A	B	C	D	E	F	G	H	I	J	K	L	M	N[c]
	1.800	1.783	1.765	1.777	1.765	Q_{os}	Q_{ow}	no Q	Q_{os}	no QH_2	Q	QH_2	Q	%
WT	98.3	0.0	1.7	98	2	0.98	0.98	0.02	0.98	0.02	≤1.6[d]	≤1.6[d]	≤1.6[d]	100
F144														
Y	95.0	0.0	5.0	96	4	0.95	0.95	0.05	0.96	0.04	≤1.6	≤1.6	≤1.6	92
W	96.9	1.6	1.5	92	8	0.98	0.97	0.02	0.92	0.08	≤1.6	2.9	≤1.6	94
S	37.6	52.4	10.0	72	28	0.90	0.38	0.10	0.72	0.28	3.4	11.7	50.0	30
T	24.3	55.0	20.7	68	32	0.79	0.24	0.21	0.68	0.32	8.0	14.8	93.5	17
V	27.1	62.5	10.3	65	35	0.90	0.27	0.10	0.65	0.35	3.5	16.2	81.0	32
I	25.2	52.9	21.9	69	31	0.78	0.25	0.22	0.69	0.31	8.4	13.4	89.0	28
N	20.4	60.7	18.9	–	–	0.81	0.20	0.19	–	–	7.1	–	117.0	26
G	0.0	39.1	60.9	45	55	0.39	0.00	0.61	0.45	0.55	46.8	36.6	$>10^3$	4
L	1.1	12.2	86.7	5	95	0.13	0.01	0.87	0.05	0.95	201.0	570	$>10^3$	3
G158														
A	96.5	0.1	3.4	95	5	0.97	0.97	0.03	0.95	0.05	≤1.6	≤1.6	≤1.6	96
S	35.5	51.6	12.6	80	20	0.87	0.36	0.13	0.80	0.20	4.5	7.5	54.2	32
P	21.0	67.6	11.4	–	–	0.89	0.21	0.11	–	–	3.7	–	112.8	14
C	1.0	35.9	64.0	–	–	0.37	0.01	0.64	–	–	51.8	–	$>10^3$	6
V	2.3	13.0	84.7	8	92	0.15	0.02	0.85	0.08	0.92	170.0	345.0	$>10^3$	0
L	3.4	14.1	79.1	15	85	0.18	0.03	0.79	0.15	0.85	132.0	170.0	$>10^3$	0
I	4.9	12.4	82.7	5	95	0.17	0.05	0.83	0.05	0.95	146.4	570.0	$>10^3$	0
W	2.0	5.0	93.0	8	92	0.07	0.02	0.93	0.08	0.92	398.6	345.0	$>10^3$	0
N	3.6	7.6	88.8	12	88	0.11	0.04	0.89	0.12	0.88	242.7	220.0	$>10^3$	0

[a] The results presented in this table are from the analysis of EPR spectra (Figures 4 and 5) obtained from chromatophores from a single batch of cells of each mutant strain. Dashed boxes indicate that the data was not determined. [b] K_D values are determined from Q_o site occupancies as described in the Materials and Methods. K_D values for F144Y, F144W, and G158A are too small to measure and are given an upper limit. In some other mutants, K_D values are too large to be estimated and are given a lower limit. [c] Cyt bc_1 complex relative activities were determined at a redox potential of 100 mV. In each mutant, the initial slope of flash activated cyt *b* reduction (antimycin present) was compared to that of the wild type (100). [d] K_D values for the wild type have been directly determined by measuring the occupancies of the Q_{os} and Q_{ow} domains of the Q_o site in chromatophore membranes containing varied amount of ubiquinone (Ding et al., 1992). The determined K_D value of the Q_{os} domain for Q or QH_2 is 0.05 mM, while the K_D value of the Q_{ow} domain for Q is 0.9 mM in the wild type.

describes the same interaction between the Q_{os} domain and the QH_2 of the Q_{pool}. It follows that QH_2 binds strongly and exchanges slowly with the Q_{os} domain of the Q_o site.

(b) Reaction Rates, (i) Measurement. Table 2, column E, shows the rates of the first QH_2 oxidation when the Q_{pool} was virtually all QH_2 prior to activation. The wild-type rate was measured to be 1620 s^{-1}. Mutants F144W and G158A displayed rates comparable with the wild type strain, F144S and I, and G158S were 4−5-fold slower, F144G was 18-fold slower, and G158W was >300-fold slower (too slow to measure). Table 2, column F, shows the rate of the first QH_2 oxidation when the Q_{pool} was all Q before activation. Under these conditions the rates for the wild type and each mutant were generally 5−12-fold slower than when the Q_{pool} was fully QH_2.

Table 2, column G, shows the rates of the second QH_2 oxidized, measured when the Q_{pool} was all QH_2 prior to activation. These are generally slower than the first QH_2 oxidized under the same conditions. The second QH_2 oxidation rate measured when the Q_{pool} was all Q rather than all QH_2 prior to activation was again ≥10-fold slower, but details of the rates are not presented here due to the complications mentioned under Materials and Methods.

(ii) Provisional Assignment of Reaction Rates to Rapid Exchange of Q and QH_2, between the Q_{ow} Domain and Q_{pool}. The interaction of the Q_{ow} domain with Q and QH_2 is expected to contrast with that in the Q_{os} domain not only in the characteristic of weaker binding but also in an exchange that is rapid relative to the catalytic turnover rate. The simplest application of eq 5 in Materials and Methods for the determination of K_D values from reaction rates is for the first QH_2 oxidized when there is only QH_2 present at the time of activation (Table 2, column E). Figure 8B presents the expressions graphically with guidance from a value for the k_{cat} of 1700 s^{-1}, chosen slightly higher than the 1620 s^{-1} measured for the wild type rate. The calculated K_{DQH_2} (rate) values are listed in Table 2, column H.

Comparisons between the collected K_D values in Table 3 show that the provisionally assigned Q_{ow} domain K_{DQH_2} (rate) values are consistently similar to the proposed companion K_{DQ} (EPR) values obtained for the Q_{ow} domain in the wild type and various mutants. If the provisional assignment of the K_{DQH_2} (rate) values to the Q_{ow} domain is correct, this provides an alternative way of measuring the K_{DQH_2} value for the Q_{ow} domain, not possible by EPR analysis.

Redox Midpoint Potentials of the Q/QH_2 Couples in the Q_{os} and Q_{ow} Domains

(i) Redox Midpoint Potentials from the K_D Values. The K_D values of both Q and QH_2 in the Q_{os} and Q_{ow} domains from the different F144 and G158 mutants allow the calculation of the E_{m7} values for the Q/QH_2 redox couple in each domain (eq 6). Table 4 shows that the calculated E_{m7} values fall within the 70−95 mV range and in no case is there a large deviation from that of the Q_{pool} (E_{m7} = 90 ± 10 mV). The up to 20 mV lowering effect on the Q_{os} and Q_{ow} domain E_{m7} values reflects the general trend of the site having a somewhat enhanced affinity for Q over QH_2.

In a limited number of cases, redox potentiometry combined with EPR, as described in the *Redox Midpoint Potentials of the Q_o Site Q/QH_2 Couples* under Materials

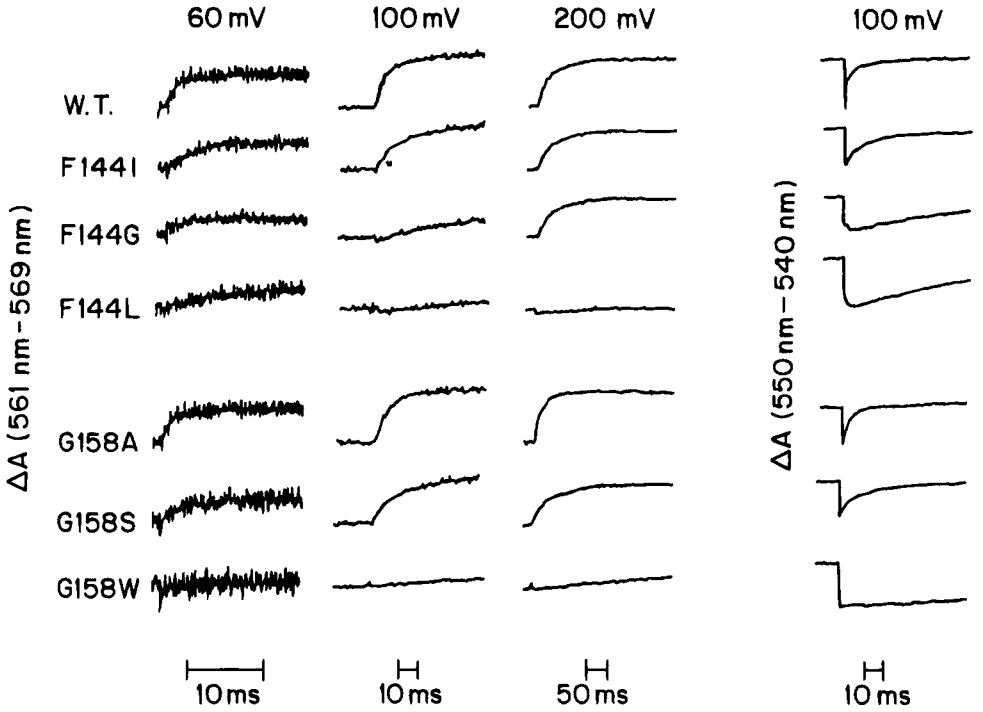

FIGURE 6: Kinetics of QH_2 oxidation in the cyt bc_1 complex from the wild type and selected mutants. Chromatophores from wild type and selected mutants were suspended in 100 mM KCl and 50 mM MOPS, pH 7.0, at a concentration of 0.1 μM cyt bc_1 complex. Kinetics for the first QH_2 oxidation (monitoring cyt b_H reduction) were measured at three redox potentials (60 ± 10, 100 ± 10, and 200 ± 10 mV) in the presence of the Q_i site inhibitor antimycin. Kinetics for the second QH_2 oxidation (monitoring cyt c re-reduction) were measured at the redox potential of 100 ± 10 mV in the absence of Q_i site inhibitor antimycin. The time course of the amplitudes of the kinetic traces were recorded as follows. For the kinetics measured at redox potentials of 100 and 200 mV, traces were averaged 20 times with an interval of 1 min between flashes to allow relaxation back to the original state. For the kinetics measured at redox potential of 60 mV, traces were averaged for 10 times with an interval of 5 min between flashes. The time scales are indicated in figure.

Table 2: Yield and Rate of QH_2 Oxidation in the Q_o Site of the Mutants[a]

	reaction yield				reaction rate (s^{-1})			
	first QH_2		second QH_2	$K_{D(yield)}$ (mM)	first QH_2		second QH_2	$K_{D(rate)}$ (mM)
	A	B	C	D	E	F	G	H
Q_{pool}	QH_2	Q	QH_2	QH_2	QH_2	Q	QH_2	QH_2
WT	1.00	1.00	1.00	<0.5	1620	152	353	1.5
F144W	0.95	0.96	1.00	1.6	1470	150	380	4.5
F144S	0.81	0.85	0.76	7.0	310	55	230	135
F144I	0.74	0.72	0.71	10.5	295	47	195	140
F144G	0.41	0.35	0.48	43.2	95	9	73	510
F144L	0.23	0.20	0.21	100.4	50	3	50	>1000
G158A	1.00	0.98	1.00	<0.5	1530	154	325	3.3
G158S	0.89	0.88	0.83	3.7	241	52	160	180
G158W	0.00	0.00	0.04	>1000	0	0	8	>1000

[a] The results presented in this table are from the analysis of kinetics (Figure 6) performed on chromatophores from a single batch of cells of each mutant strain.

and Methods, was used to check these calculated E_{m7} values (eq 6) for the Q_{os} domain. Ding et al. (1992), working with the wild-type strain, determined an E_{m7} value of 80 ± 5 mV when the Q_{os} and Q_{ow} domains were fully occupied and an E_{m7} value of 95 ± 10 mV when only the Q_{os} domain was occupied. Both values are close to that of the Q_{pool} (90 ± 10 mV) and to that calculated from the K_{DQH_2} (EPR or yield) and K_{DQ} (EPR) values of the Q_{os} domain. This confirms and completes the thermodynamic cycle of the binding and redox interaction between the Q_{pool} and the Q_{os} domain. It also shows that the occupancy of the Q_{ow} domain has only a small effect on the preference of Q_{os} domain binding to Q or QH_2.

These data and conclusions are supported by analysis of F144W and F144I. F144I is noteworthy because its Q_{os} and Q_{ow} domains are partially occupied with 25% of the population having both the Q_{ow} and Q_{os} domains fully occupied, 50% having only Q_{os} domains occupied and 25% having both domains unoccupied (Table 1). Again, the E_{m7} value obtained (85 ± 10 mV) is close to the E_{m7} of the Q_{pool} and to the value derived from the K_D values for the Q and QH_2 in the Q_{os} domain (Table 4); the data for the redox titration data is not presented but the quality is the same as shown in Ding et al. (1992). Finally, as a control for the redox titration method, the mutant F144L with less than 20% occupancy of the Q_{os} was examined, and, as expected, the EPR spectrum of F144L was dominated by the g_x band at 1.765 over the entire redox potential range covered. This result is the same as that presented by Ding et al. (1992) for a wild-type Q_o site rendered virtually devoid of Q/QH_2 by solvent extraction.

(ii) Apparent Redox Midpoint Potentials from Kinetics. Table 4 lists the apparent E_{m7} values drawn from the redox titration of the rates of the first and second QH_2 oxidation reactions measured at the redox potential from 40 to 230 mV. Although the basis of the rate change as the Q_{pool} is changed from all QH_2 to all Q prior to flash activation is not understood in any detail, it is clear that the apparent E_{m7} values do not deviate far from one another or from that of the Q_{pool}. As such, they are consistent with the four K_D values of the Q and QH_2 at the Q_{os} and the Q_{ow} domains reported here. It is worth noting that the first QH_2 oxidation indicates an E_{m7} value higher, and the second QH_2 oxidation somewhat lower, than that of the Q_{pool}. Such deviations deserve further investigation.

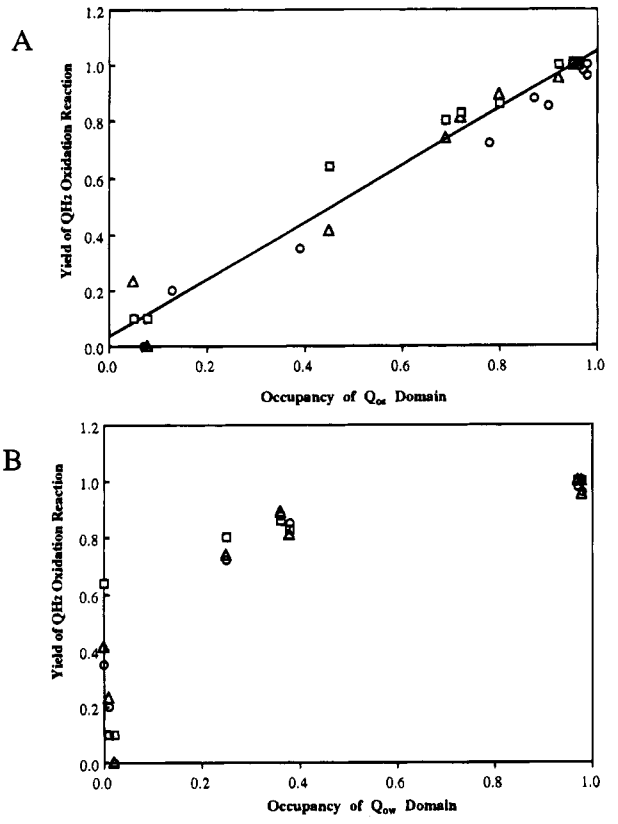

FIGURE 7: Correlation of the equilibrium Q/QH_2 occupancies of the Q_{os} and Q_{ow} domains and the flash induced yield of the QH_2 oxidation in the Q_o site. The yield of QH_2 oxidation in the Q_o site from various mutants relative to that of the wild type are listed in Table 2. They are plotted as a function of the occupancy of the Q_{os} domain (part A) or Q_{ow} domain (part B) determined by EPR and listed in Table 1. The first QH_2 oxidation yield was measured when the redox potential was poised at 200 mV (○) or 100 mV (△). The second QH_2 oxidation yield was measured when the redox midpoint potential was poised at 100 mV (□).

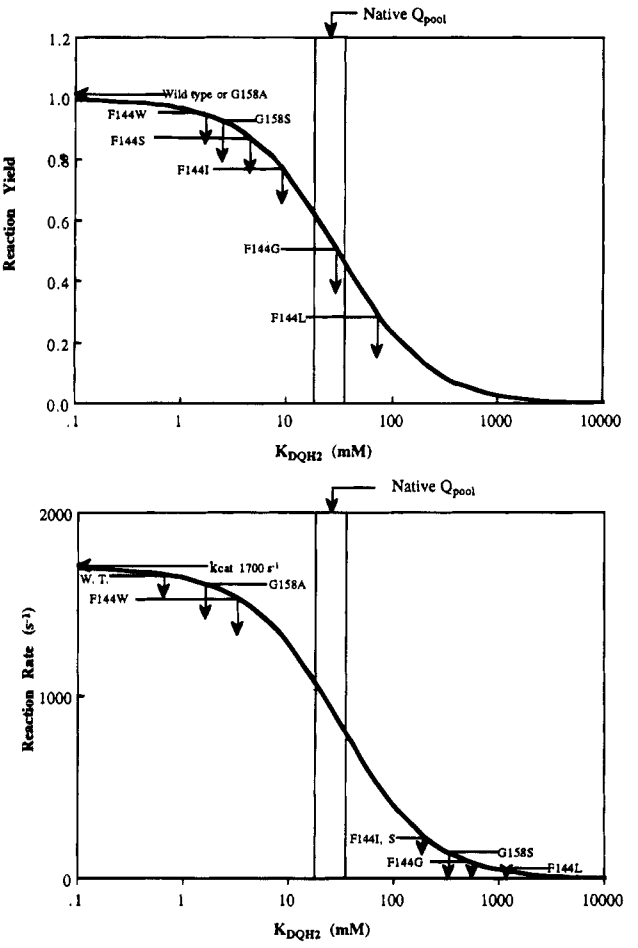

FIGURE 8: Determination of the K_{DQH_2} values of the Q_{os} and Q_{ow} domains from the relative yield and rate of the QH_2 oxidation in the Q_o site. The relative yields and rates of QH_2 oxidation for the wild type and mutants are listed in Table 2. Part A describes the determination of the K_{DQH_2} values from the relative yield of QH_2 oxidation. The solid line represents eq 4, where the measured relative yield represents the fraction of the Q_o site occupied and [Q] is the Q_{pool} concentration, 30 ± 6 mM, as indicated. The arrows indicate the K_{DQH_2} values corresponding to the QH_2 oxidation yields displayed by the various mutants. Part B shows the determination of the K_{DQH_2} values from the QH_2 oxidation rate. The solid line is the graphical representation of the eq 5 relationship between the K_{DQH_2} values in the Q_o site domain and the QH_2 oxidation rates (K_{obs}). Arrows indicate the apparent K_{DQH_2} values corresponding to the QH_2 oxidation rates displayed by the various mutants

DISCUSSION

In this study, two families of neutral aromatic and aliphatic mutants of F144 and G158 in the cyt *b* polypeptide of *R. capsulatus* cyt bc_1 complex have provided a wide range of binding affinities for Q and QH_2 at the Q_{os} and Q_{ow} domains in the Q_o site. Changing only the binding affinities without affecting the Q_o site redox properties or the k_{cat} value, these families have provided a well quantified and perhaps unique perspective on the primary steps of energy conversion in the parent wild type cyt bc_1 complex. The following discussion therefore focuses most attention on the Q_o site function of the wild type cyt bc_1 complex.

The Q_{os} and Q_{ow} Domains in the Q_o Site Are Contiguous

The present investigation shows that the earlier recognized two ubiquinone molecules in the Q_{os} and Q_{ow} domains of the Q_o site (Ding et al., 1992) are essential for energy conversion in the cyt bc_1 complex. One of the remarkable results is the finding that *single* neutral substitution at either F144 or G158 of the cyt *b* polypeptide weakens the affinity of both the Q_{os} and Q_{ow} domains to approximately the same extent relative to the overall >1000-fold range of change. The similar effect on both the Q_{os} and Q_{ow} domains from a single mutation complements the earlier indication that only one Q_o site inhibitor molecule (stigmatellin or myxothiazol) can eliminate both ubiquinone molecules from the Q_o site (Ding et al., 1992). It would appear then that the Q_{os} and Q_{ow} domains in the Q_o site are part of a contiguous binding cavity, and that the occupying ubiquinone molecules are in physical contact, one ubiquinone contributing to and being dependent on the binding of the other. One illustrative view of such an arrangement could be that the residues F144 and G158 are part of the stronger Q/QH_2 binding Q_{os} domain and any effect on the Q_{os} domain incurred by mutation has a similar effect on the weaker Q/QH_2 binding Q_{ow} domain. This arrangement of the pair of ubiquinones has the potential to confer special catalytic properties on the QH_2 oxidation process in the Q_o site.

Redox Properties of the Q_{os} and Q_{ow} Domains

The Q_{os} and Q_{ow} domain E_{m7} values for the Q/QH_2 couples in the wild type and the mutants presented here, either measured directly or calculated from the K_D values, fall

Table 3: K_D Values of the Q_{os} and Q_{ow} Domains of Q_o Site[a]

	Q_{os} domain			Q_{ow} domain	
	$K_{D(EPR)}$ (mM)		$K_{D(yield)}$ (mM)	$K_{D(EPR)}$ (mM)	$K_{D(rate)}$ (mM)
Q_{pool}	Q	QH_2	QH_2	Q	QH_2
WT	≤1.6 (0.05)	≤1.6 (0.05)	<0.5	≤1.6 (0.9)	2 ± 1
F144W	≤1.6	3 ± 1	1 ± 0.5	≤1.6	5 ± 2
F144S	3 ± 1	12 ± 2	5 ± 2	50 ± 15	135 ± 50
F144I	8 ± 2	15 ± 3	12 ± 4	95 ± 24	143 ± 25
F144G	47 ± 5	37 ± 5	56 ± 10	≥1000	510 ± 45
F144L	200 ± 35	570 ± 60	100 ± 30	≥1000	990 ± 100
G158A	≤1.6	≤1.6	<0.5	≤1.6	4 ± 2
G158S	4 ± 1	7 ± 3	4 ± 2	55 ± 15	180 ± 30
G158W	440 ± 50	350 ± 45	>1000	≥1000	≥1000

[a] The data presented are average values and standard deviations from EPR and kinetic analyses calculated from separate experiments done on chromatophores from three separate batches of cells of each mutant strain.

Table 4: E_{m7} Values (mV) of Q/QH_2 in the Q_{os} and Q_{ow} Domains of Q_o Site

		F144						G158	
	WT	W	S	T	V	I	G	A	S
Q_{os}									
from K_{DQ}/K_{DQH_2}[a]	90	83	74	82	70	84	93	90	88
from EPR[b]	95 (85)[c]	92	–	–	–	84	–	–	–
Q_{ow}									
from K_{DQ}/K_{DQH_2}[d]	80	75	77	–	–	85	99	78	75
from redox titration of first QH_2 oxidation rate	112	105	–	–	–	134	–	110	104
from redox titration of second QH_2 oxidation rate	98	80	69	79	72	70	75	103	85

[a] E_{m7} values are calculated from the K_{DQ} and K_{DQH_2} values in Table 3. [b] E_{m7} values are determined from the redox titration of the g_x band of the [2Fe-2S] EPR spectrum. [c] In the wild type, the E_{m7} for the Q_{os} domain is 85 ± 10 mV when only Q_{os} domain binds Q and is 95 ± 10 mV when both the Q_{os} and Q_{ow} domains bind Q [see Ding et al. (1992)]. [d] E_{m7} values are calculated from the K_{DQ} and K_{DQH_2} values shown in Table 3. Symbols (–) in table indicate that data were not determined.

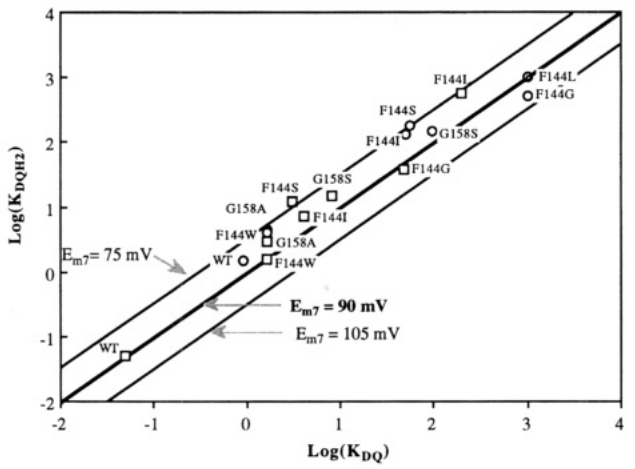

FIGURE 9: Comparison of the K_{DQ} and K_{DQH_2} values from the Q_{os} and Q_{ow} domains of the Q_o site and their relationship with E_{m7} values. The bold line drawn through the data points according to eq 6 represents the situation where K_{DQH_2} and K_{DQ} are equal, and hence the E_{m7} value of the Q_o site Q/QH_2 couple is the same as the Q_{pool} (90 mV). The parallel limits (90 ± 15 mV) indicate the extent of the variance of the E_{m7} values for the Q_o site Q/QH_2 couple of the individual mutants of the family.

within a small range around that of the Q_{pool} (E_{m7} = 90 ± 10 mV) (Table 4). If anything, the values are on the low side, consistent with an up to 3-fold higher affinity of Q relative to QH_2. These variances in the K_D values and the resultant E_{m7} values are summarized in Figure 9. It appears that neither domain plays any role in altering, for some catalytic purpose, the basic two-electron *equilibrium* redox properties of the individual Q/QH_2 couples away from that seen in the Q_{pool} (Ding et al., 1992). This rather plain result shows that the binding affinity for the ubiquinone pair in the Q_{os} and Q_{ow} domains comes from forces that do not significantly discriminate between Q and QH_2. This may be achieved, for instance, by the atomic level interactions being predominantly directed to the packing of the ubiquinone ring and the methoxyls (Gunner et al., 1985; Warncke & Dutton, 1993a,b) or the first one or two isoprene substituents (McComb et al., 1990; Warncke et al., 1994). However, if the interaction does include the keto/phenolate oxygen atoms themselves, as is the case for the Q/QH_2 in the Q_A and Q_B sites of the reaction center (McComb et al., 1990; Warncke et al., 1994; Ermler et al., 1994), then the interaction strength for each structure must be the same to within a fraction of a kcal/mol. This, for instance, can be envisaged as occurring uniquely through hydrogen-bond donation from protein to an available lone pair of the keto or phenolate oxygens, the basicity of which remains unaltered in each form (Keske et al., 1990). A further important consequence of the similarity between the E_{m7} values of Q/QH_2 in the two domains is the absence of any pronounced specific cooperative redox state interaction between Q and QH_2 in the adjacent domains. Such cooperative interactions would lead to splitting in the redox energy levels of the two Q/QH_2 couples that would be seen in the redox titrations well described for dimers (Clark, 1960). The existence of splitting would have indicated that the Q_o site would stabilize the presence of one Q and one QH_2 in the Q_{os} and Q_{ow} domains. Again, this is clearly not the case for the ubiquinone pair in the domains of the Q_o site, and we can say that if there is a Q in one domain then there is no preference to bind QH_2 over Q in the other domain.

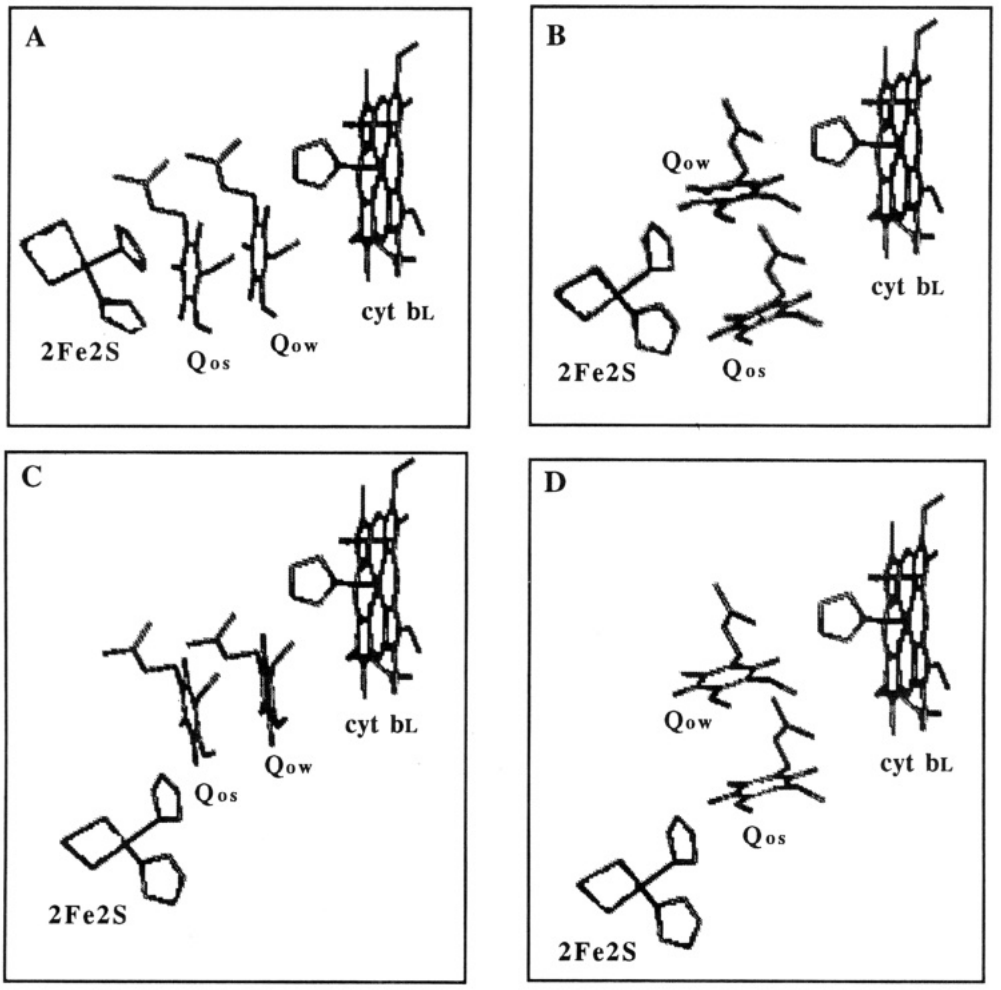

FIGURE 10: Possible arrangements of the ubiquinone occupants in the Q_{os} and Q_{ow} domains in the Q_o site relative to the oxidants, [2Fe-2S] cluster, and cyt b_L heme of the cyt bc_1 complex. Part A shows the Q_{os} domain ubiquinone oxygens positioned to receive hydrogen-bond donations from each ϵ-nitrogen of two histidine imidazoles of the [2Fe-2S] cluster (Gurbiel et al., 1991; Davidson et al., 1992; van Doren et al., 1993; Ohnishi et al., 1994), while one of the oxygens of the ubiquinone in the Q_{ow} domain receives one hydrogen bond from the δ-nitrogen of the histidine imidazole of the cyt b_L. Part B shows the Q_{ow} domain positioned to receive hydrogen-bond donations from both the [2Fe-2S] cluster and cyt b_L histidines, while the Q_{os} domain ubiquinone receives one hydrogen bond from the [2Fe-2S] cluster. Parts C and D present two other arrangements with only single hydrogen bonds from the [2Fe-2S] cluster and cyt b_L to each of the Q_{os} domain and Q_{ow} domain ubiquinones. These arrangements extend the possible distance between the [2Fe-2S] cluster and the cyt b_L and permits the [2Fe-2S] cluster to be placed well outside of the lipid tail part of the membrane profile as indicated by Figure 1.

Structural Models of the Ubiquinones in the Q_{os} and Q_{ow} Domains

Figure 10 presents four variants of a working model of the ubiquinones in the Q_{os} and Q_{ow} domains of the Q_o site based on the original suggestion shown in Figure 8 of Ding et al. (1992). Each variant attempts to arrange the two ubiquinone binding domains with respect to the [2Fe-2S] cluster and the cyt b_L heme in a manner that is consistent with (a) the [2Fe-2S] EPR spectral phenomena, (b) the higher affinity of the Q_{os} domain over the Q_{ow} domain and the cooperative nature of the binding reactions, and (c) the position of the cofactors with respect to the membrane dielectric profile (Glazer & Crofts, 1984; Robertson & Dutton, 1988). From the available EPR spectral responses, it is most logical to suggest that the ubiquinone in the Q_{os} domain has a more intimate association with the [2Fe-2S] cluster. Figure 10 suggests that the two quinone molecules are stacked cofacially as in a "quinhydrone" structure but with the exception of model B they could equally be positioned edge to edge, affording a greater distance between the [2Fe-2S] cluster and cyt b_L as shown in Figure 13. In all the cases, for reasons that will become clearer below, we propose that the two domains are functionally arranged to promote a linear sequence of electron transfer between the [2Fe-2S] cluster and cyt b_L as follows:

$$[2Fe\text{-}2S] \rightarrow Q_{os} \rightarrow Q_{ow} \rightarrow \text{cyt } b_L$$

Different Functional Roles for the Ubiquinones of the Q_{os} and Q_{ow} Domains

In the wild type strain, the K_D values for QH_2 or Q in the Q_{os} domain (0.05 mM) are some 20-fold smaller than the corresponding values for the Q_{ow} domain (0.9 mM) (Ding et al., 1992). These K_D values together with the prevailing Q_{pool} concentration (30 $\pm$ 6 mM) dictates that both domains are nearly fully occupied at equilibrium (Ding et al., 1992). The results presented here provide compelling evidence that the ubiquinones of the Q_{os} and Q_{ow} domains serve in different functional capacities. It is clear that the strongly ubiquinone binding Q_{os} domain must be occupied by QH_2 or Q for the Q_o site to be functional, but, in contrast to our earlier suggestion (Ding et al., 1992), the new evidence indicates

that there will be no significant exchange of QH_2 or Q from the Q_{os} domain with the Q_{pool} as an obligate part of a catalytic cycle. On the other hand, the weaker binding ubiquinone Q_{ow} domain is, as before, viewed as being open for rapid exchange of Q or QH_2 with the Q_{pool} and as such appears to be the domain that brings in the substrate QH_2 and releases the product Q.

Possible Reaction Sequences in the Q_o Site

Conditions in the wild type which, upon activation, lead to an QH_2 oxidation rate that approaches the k_{cat} value (1700 s^{-1}) are

(a) oxidized [2Fe-2S] → QH_2 (Q_{os}) → QH_2 (Q_{ow}) → oxidized cyt b_L

We proposed that the sequence for the first QH_2 oxidation, involving semiquinone states (designated SQ without identifying the protonation state) is

(b) reduced [2Fe-2S] → SQ → QH_2 → oxidized cyt b_L

(c) reduced [2Fe-2S] → QH_2 → SQ → oxidized cyt b_L

(d) reduced [2Fe-2S] → QH_2 → Q → reduced cyt b_L

At this point, there are two possibilities for the second QH_2 oxidation, which occurs at a rate of approximate 350 s^{-1} in the wild type strain. Which possibility prevails depends on whether reactivation occurs before or after the Q_{ow} domain exchanges Q for a new QH_2 from the Q_{pool}. Reactivation requires the reoxidation of the [2Fe-2S] cluster by cyt c_1 [this can occur at least at 10^5 s^{-1} (Meinhardt & Crofts, 1983; Crofts & Wang, 1989)] and the reoxidation of the cyt b_L by cyt b_H [this has been estimated from cyt b_L kinetics to be $>10^4$ s^{-1} (Crofts & Wang, 1989)]. It seems likely that both possibilities will occur depending on the prevailing conditions of reduction of the Q_{pool} or the light intensity during bacterial growth *in vivo*.

In the first possibility, when in "d" the exchange of the Q_{ow} domain Q for a new QH_2 from the Q_{pool} occurs before reactivation, the system returns to "a" for the second QH_2 oxidation and the cycle repeats.

In the second possibility, when "d" is reactivated for the second QH_2 oxidation before exchange of Q for a new QH_2 in the Q_{ow} domain will result in the generation of

(e) oxidized [2Fe-2S] → QH_2 → Q → oxidized cyt b_L

and the process will be followed by a new sequence, which we propose is

(f) reduced [2Fe-2S] → SQ → Q oxidized cyt b_L

(g) reduced [2Fe-2S] → Q → SQ → oxidized cyt b_L

or

(f′) oxidized [2Fe-2S] → SQ → SQ → oxidized cyt b_L

to produce

(h) reduced [2Fe-2S] → Q → Q → reduced cyt b_L

This second possibility is the sequence that was described in thermodynamic detail by Ding et al. (1992). In that model, after "h" the system was returned to "a" by exchange of both Q molecules for two new QH_2 molecules from the Q_{pool}. However, since as already mentioned above, we now have good reason to believe that the Q_{os} domain does not exchange with the Q_{pool} rapidly, the short term exchange by Q_{ow} domain will form "i" and then perhaps by transhydrogenation, "j"

(i) reduced [2Fe-2S] → Q → QH_2 → reduced cyt b_L

(j) reduced [2Fe-2S] → QH_2 → Q → reduced cyt b_L

and thus the system returns to "d".

Another set of the conditions studied in this report was the case where the Q_{pool} is oxidized and hence both the Q_{os} and Q_{ow} domains are occupied by Q before activation. Thus starting with

(k) reduced [2Fe-2S] → Q → Q → oxidized cyt b_L

activation yields

(l) oxidized [2Fe-2S] → Q → Q → oxidized cyt b_L

and exchange of the Q_{ow} domain with a QH_2 from the reaction center Q_B site generates

(m) oxidized [2Fe-2S] → Q → QH_2 → oxidized cyt b_L

which then proceeds after transhydrogenation through steps "e" through "h". In the wild-type strain, the apparent rate of QH_2 oxidation under these conditions is 150 s^{-1}. This rate most likely corresponds to the exchanging process of Q in the Q_{ow} domain for QH_2 coming from the Q_B site. The studies that address this question specifically will be presented elsewhere (Ding, Moser, Daldal and Dutton, manuscript in preparation).

Q_{os} and Q_{ow} Domain Semiquinone Barriers

The above proposed sequences highlight areas for new work to obtain a more quantitative understanding of the exchange rates of the Q and QH_2 in the Q_{os} and Q_{ow} domains. They also demonstrate the vital importance of the SQ state-(s), about which we know little in the Q_o site.

The SQ has long been considered to be the key to the mechanism of the primary steps of energy conversion in the cyt bc_1 complex (Wikström & Berden, 1972; Mitchell, 1975). Early equilibrium measurements in chromatophores isolated from *Rhodobacter sphaeroides* indicated that the SQ stability constant was less than 10^{-7} in the Q_o site (Takamiya & Dutton, 1979), while pre-steady-state experiments with mitochondria revealed a kinetically trapped free-radical signal that was identified as a SQ in the Q_o site (de Vries et al., 1981).

Figure 11 suggests the barriers to the reaction sequence utilizing the Q_{os} and Q_{ow} domain SQ states to promote efficient oxidation of QH_2 coupled to the reduction of oxidized [2Fe-2S] cluster and ferri-cyt b_L. The mechanism is consistent with Mitchell's original idea (1975) which emphasized that the QH_2 oxidation is energetically highly cooperative, requiring both oxidized [2Fe-2S] cluster and ferri-cyt b_L. The figure suggests that the initiating oxidation of QH_2 by the oxidized [2Fe-2S] cluster occurs in the

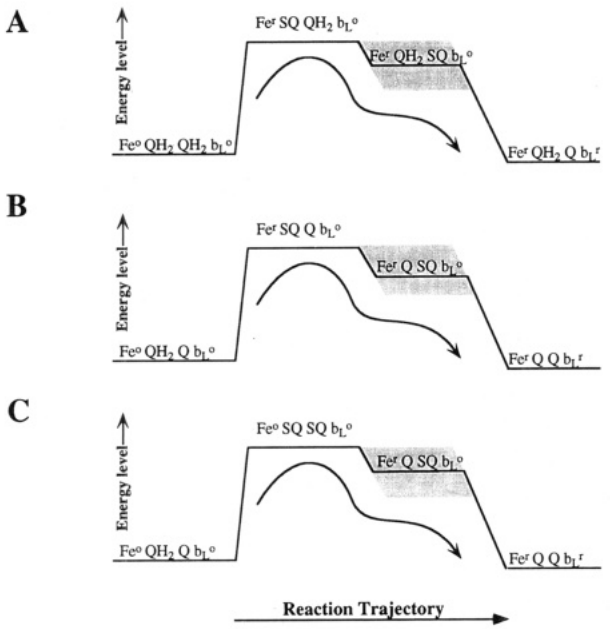

FIGURE 11: Energetic pathways of the QH_2 oxidation in the Q_o site. Part A shows the QH_2 oxidation in the Q_o site when both the Q_{os} and Q_{ow} domains are occupied by QH_2. The semiquinone (SQ) formation in the Q_{os} domain by the [2Fe2S] cluster is considered as the barrier for the QH_2 oxidation reaction. The favored SQ transfer from the Q_{os} domain to the Q_{ow} domain is the key for the unidirectionality of the electron-transfer process of the QH_2 oxidation in the Q_o site. Part B shows a similar pathway for the QH_2 oxidation in the Q_o site when only the Q_{os} or Q_{ow} domain is occupied by one QH_2 and one Q. Again, the SQ formation in the Q_{os} domain is considered as the barrier for the reaction, and the directionality of the SQ movement is the same as in part A. Part C is a derivative of the model in part B and is considered as a "quinhydrone" model. In this case, the quinhydrone formation of the QH_2 and Q in the Q_{os} and Q_{ow} domains in the Q_o site becomes the barrier for the overall reaction. The energy level of the semiquinone state in the Q_{ow} domain is presented as a shaded area under each condition, indicating that it could be anywhere within the area.

adjacent Q_{os} domain, and that it encounters a major thermodynamic barrier presented by the SQ state. Such a barrier will lower the steady-state equilibrium concentration of the reduced [2Fe-2S]-SQ state to vanishingly low levels, thereby greatly diminishing the possibility of wasteful competing reactions. The height of the barrier will be governed by the degree of instability of the SQ state. The figure suggests that the height of the SQ barrier of the Q_{os} domain proximal to the [2Fe-2S] cluster might be higher (smaller stability constant) than the one in the distal Q_{ow} domain. In this way, a SQ state formed in the Q_{os} domain is promoted to a lower, yet still unstable state in the more distant Q_{ow} domain before reducing ferri-cyt b_L. The overall reaction is expected to have a substantial activation energy, and, indeed, this has been shown to be the case. Values in the range of 8−12 kcal/mol from 40 to −10 °C (K. M. Petty and P. L. Dutton, unpublished determinations) for the QH_2 oxidation reaction have been obtained in *R. sphaeroides*, which are consistent with the recent measurements by Crofts and Wang (1989), who obtained 7.9 kcal/mol from 40 to 10 °C under a variety of conditions. These points are presented more quantitatively in Figure 12 and are detailed below.

(i) A Sequential SQ Barrier Model. In the initial step involving the [2Fe-2S] cluster oxidation of QH_2 in the Q_o site, we suggest a reasonable E_{m7} value for the QH_2/SQ in

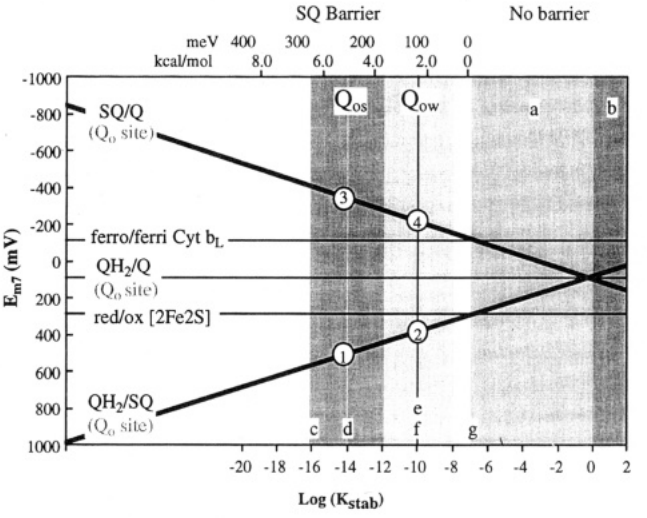

FIGURE 12: Semiquinone stability constants in the Q_{os} and Q_{ow} domains of the Q_o site. The SQ stability constant is related to the redox midpoint potentials of the QH_2/SQ and SQ/Q as expressed in eq 8. The E_{m7} values of the single-electron oxidants ([2Fe-2S] cluster and cyt b_L) are also shown for comparison. The magnitude of the SQ barrier for the reaction of the QH_2 to SQ by the [2Fe-2S] cluster is indicated on the top of the figure. In region a, the SQ is thermodynamically stable. In region b, the SQ can be favorably formed directly by the oxidized [2Fe2S] cluster, i.e., a negative barrier for the reaction. Region **c** is the upper limit of the SQ stability constant in the Q_o site directly measured by EPR (Takamiya & Dutton, 1979). Region d is the SQ stability constant estimated for the Q_{pool} (Mitchell, 1975). Regions e and f are suggested to be the most likely range for SQ stability constants for the Q_{ow} and Q_{os} domains, respectively. Region g indicates the low limit of the SQ stability constant in the Q_{os} domain, as suggested by Crofts and Wang (1989), but the system could still work even at lower values.

the Q_{os} domain of +520 mV (circled 1 in Figure 12). This SQ level contributes +230 meV (+5.3 kcal/mol) to the barrier and hence an unfavorable equilibrium constant of 10^{-4} for SQ formation in the Q_{os} domain. An E_{m7} value of +520 mV for the QH_2/SQ couple taken together with the measured E_{m7} value for the QH_2/Q couple in the Q_{os} domain (+90 mV; Table 4) allows the calculation of the E_{m7} value for the companion SQ/Q couple to be −340 mV (circled 2 in Figure 12) as derived from

$$E_{m7} = (E_{m7(QH_2/SQ)} + E_{m7(SQ/Q)})/2 \qquad (7)$$

and thus the SQ stability constant is close to 10^{-14} according to

$$\log K_{stab} = (E_{m7(QH_2/SQ)} - E_{m7(SQ/Q)})/60 \qquad (8)$$

The second step involves the transfer of the SQ from the Q_{os} domain to the Q_{ow} domain. Here there are two possibilities indicated by Figures 11A,B. If the reaction sequence proceeds as in steps a−d, starting with QH_2 in both the Q_{os} and Q_{ow} domains (Figure 11A), we propose that the transfer of the SQ from the Q_{os} to Q_{ow} domain is achieved by virtue of a lower E_{m7} value of the QH_2/SQ in the Q_{ow} domain compared to that in the Q_{os} domain. In essence, the SQ formed in the Q_{os} domain will oxidize the QH_2 in the Q_{ow} domain. For example, if we suggest an E_{m7} value of +400 mV for the Q_{ow} domain QH_2/SQ, then the reaction (circled 3 in Figure 12) for the movement of SQ from the Q_{os} to the Q_{ow} domain will be favored ($\Delta G^\circ = -120$ meV) while still maintaining a significant barrier. An E_{m7} value

for the QH_2/SQ of +400 mV together with the measured E_{m7} value for the QH_2/Q couple in the Q_{ow} domain (+80 mV; Table 4) provides (from eq 7) an E_{m7} value for the companion SQ/Q of −240 mV (circled 4 in Figure 12) and a stability constant in the region of 10^{-10} (from eq 8).

If the reaction sequence proceeds as in steps e−h starting with QH_2 in the Q_{os} and Q in the Q_{ow} domains (Figure 11B), then in this case the SQ formed in the Q_{os} domain (−340 mV) is transferred to the Q_{ow} domain favorably ($\Delta G°$ = -100 meV) in essence by reducing the Q in the Q_{ow} domain (−240 mV). It is worth noting that while the reaction pathways illustrated in Figure 11A,B and quantitated in Figure 12 may be different, the character of the barrier is predicted to be essentially the same.

The third and final step, like the first step, is common to all cases and involves the reduction of the ferri-cyt b_L (E_{m7} = −90 mV). With an E_{m7} value for the SQ/Q −240 mV in the Q_{ow} domain, this reaction is strongly favored with an equilibrium constant of slightly more than 10^2 ($\Delta G° = -150$ meV), driving the electron onto cyt b_L.

A consequence of the low stability SQ involvement in the barriers is a weak binding affinity for the Q_o site. The affinity for semiquinone in the Q_o site can be expressed as follows;

$$\log K_{DSQ} = [\log(K_{QH_2}K_{QD})]/2 + [(P - S)/2] \quad (9)$$

where, K_{DSQ} is the dissociation constant for semiquinone; K_{DQH_2} and K_{DQ} are the dissociation constants for the QH_2 and Q, respectively; the terms P and S are the logarithms of the semiquinone stability constants in the Q_{pool} and in the Q_o site, respectively. If we take the above semiquinone stability constants of 10^{-14} and 10^{-10} for the Q_{os} and Q_{ow} domains, and 10^{-10} for the Q_{pool} as estimated by Mitchell (1975), the calculated dissociation constants for semiquinones in the Q_{os} and Q_{ow} domains are 5 and 1 mM, respectively. These values indicated that, under equilibrium conditions, there will be a strong tendency for semiquinones to leave the domains. Such wasteful action is clearly guarded against, not only by very low steady-state levels of SQ but also by the rapid interdomain reaction leading to the reduction of ferri-cyt b_L.

(b) A Quinhydrone−Semiquinone Barrier Model. The close structural arrangement of the Q_{os} and Q_{ow} domains in the Q_o site invites the serious consideration that the ubiquinone pair may adopt the much studied quinhydrone state [see Foster and Foreman (1974)] in its mechanism as follows:

$$Q{-}QH_2 = QH_2{-}Q = SQ{-}SQ$$

The structural examples of Figure 10 serve to illustrate the required ring overlapping character of the quinhydrone pair ($Q{-}QH_2$). The quinhydrone is indicated in the reaction sequences delineated above in which reaction f′ is offered as an alternate to f or both f and g. The state described by f′ will replace f in the initial barrier in Figure 11C as shown, but if the oxidation of the two SQ in f′ is simultaneous, the barrier is simplified and the second level of the barrier (i.e., g) will be by-passed. At present, there are no indications that the quinhydrone state is functional. Moreover, as already mentioned, the rather similar binding properties of Q and QH_2 in the Q_{os} and Q_{ow} domains do not overtly indicate the presence of any tendency to form the $Q{-}QH_2$ pair in the Q_o site. The quinhydrone offers distinct spectral forms (Foster & Foreman, 1974) that may be worth searching for, but, as with the SQ in the sequential mechanism, the SQ−SQ state is likely to be present at vanishingly small levels. A similar quinhydrone mechanism for the operation of the Q_o site for the QH_2 oxidation has been independently suggested for the steady-state reaction in the cyt bc_1 complex (Dr. U. Brandt, personal communication).

Protolytic and Hydrogen Transfer Reactions

Very little is known about the protolytic reactions associated with the Q_o site (Petty & Dutton 1976; Jackson, 1988; Brandt & Trumpower, 1994). Clearly, the distribution of acid−base amino acid side chains, both within the Q_o site as well as outside it toward the aqueous phase, can be critical in influencing the magnitude of the barrier heights and the overall reaction kinetics and hence be additionally important in conferring directional specificity on this vectorial catalysis. As is evident in the reaction sequences discussed above, we consider it most probable that oxidation of QH_2 in the Q_{os} domain by the [2Fe-2S] cluster produces the SQ anion and that both protons are released from the electron transfer system at this point. This proposal is based on prevailing evidence from extensive equilibrium oxidation−reduction/acid−base analysis of adjacent redox cofactors, detailed as follows: The cyts c_2 and c_1 do not possess pK values that differ significantly on the ferri- or ferro- forms (Prince & Dutton, 1977) within the physiological pH range and so are not expected to undergo proton exchange coupled to oxidation and reduction. In contrast, the [2Fe-2S] cluster has a pK of 8.0 at equilibrium on the oxidized form (Prince & Dutton, 1976; Link et al., 1992), and hence, above pH 8, a single proton is expected to exchange upon oxidation and reduction. However, because the E_m value of the [2Fe-2S] cluster above this pK would remain maximally at +280 mV independent of pH, the ferri cyts c_2 and cyt c_1 (E_m values 340 and 280 mV) are still able to oxidize the [2Fe-2S] cluster above pH 8, with or without protons being released. An analogous situation exists for the reduction of cyt b_L. A ferro cyt b_L pK at 7.5 (Petty et al.,1979; Meinhardt & Crofts, 1983) yields a lower limit of −120 mV for the E_m value. Again, reduction of cyt b_L by the Q_o site SQ is feasible (suggested E_m value −240 mV; see above) without binding a proton at pH values lower than the pK. Thus, we consider redox linked proton exchange and hydrogen transfer will be normally contained within the Q_{os} and Q_{ow} domains.

Reaction Rates and Designed Distances between the Redox Centers in the Cyt bc_1 Complex

Interdomain hydrogen exchange (transhydrogenation) as discussed above will be expected to occur between the Q_{os} and Q_{ow} ubiquinones in close contact as proposed in Figures 10 and 13 [see Cha et al. (1989)]. Similarly, the flanking electron transfers between QH_2 in the Q_{os} domain and the oxidized [2Fe-2S] cluster and between the Q_{ow} domain SQ and cyt b_L are both proposed to be bridged by a single histidine and hence take place over very short distances. If these reactions were to be governed only by nonadiabatic electron transfer, they would be expected to proceed in tens of picoseconds (Moser et al., 1992). However, the high endothermicity of the barrier to the SQ, which is perhaps enhanced by the course of proton transfer from the QH_2, is most likely to limit the observed rate of these (adiabatic)

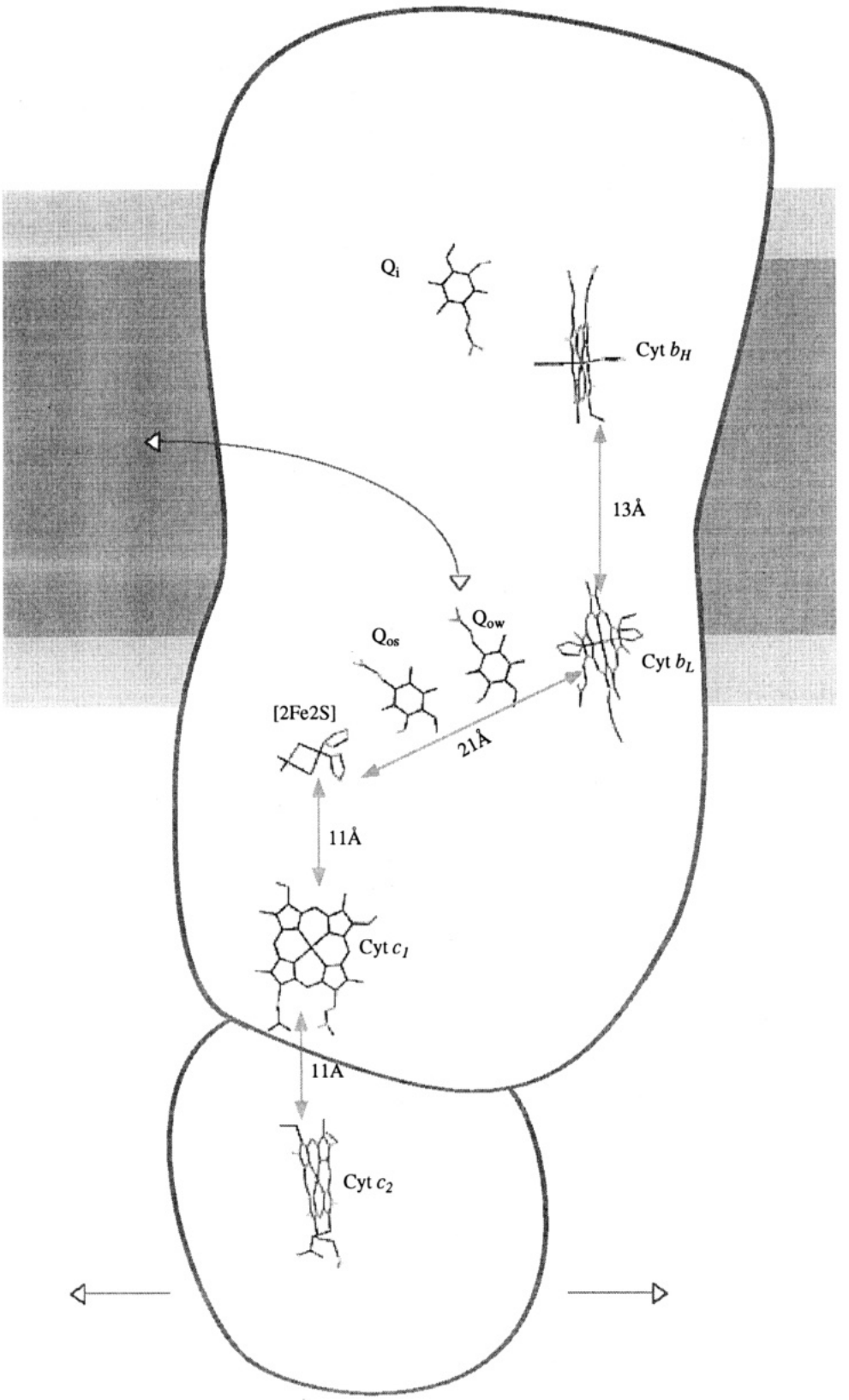

FIGURE 13: Designed electron-transfer distances between the redox centers in the cyt bc_1 complex. The basis for the organization of the redox cofactors is discussed in the text.

reactions to that of the observed k_{cat}. The k_{cat} values for the two QH_2 oxidation are relatively slow, measured to be 1700 s^{-1} for the first and 350 s^{-1} for the second QH_2 oxidation. Nevertheless, while obscured by these adiabatic rate-limited reactions, electron transfer reactions between cyt c_2, cyt c_1 and the [2Fe-2S] cluster, and between the Q_{ow} domain SQ, cyt b_L and cyt b_H, may still be governed only by nonadiabatic electron tunneling and, hence, occur at faster rates. If so, electron transfer theory places significant restraints on the possible distances between the bc_1 complex redox centers, given that productive electron transfer must be faster than unproductive electron transfer. A simple guideline to

estimating the rates of nonadiabatic electron transfer is provided by (Moser et al., 1992; Moser & Dutton, 1992)

$$\log \text{rate} = 15 - 0.6R - [3.1(\Delta G^\circ + \lambda)^2]/\lambda \quad (10)$$

where R is the edge to edge distance (Å), ΔG° is the standard free energy (negative when the reaction is favorable), and λ is the reorganization energy (positive). These reactions are discussed briefly below and the structural conclusions summarized in Figure 13.

(i) Electron Transfer between Cyt c_1 and the [2Fe-2S] Cluster. This reaction takes place with a ΔG° of near 0 meV and a rate of at least 10^5 s^{-1} (Crofts & Wang, 1989). This corresponds to an edge-to-edge distance of 11.5−13 Å with a λ estimated to be in the 700−1000 meV range. Parallel data suggest that a similar distance will prevail for the reaction between cyt c_2 bound to the cyt bc_1 complex and cyt c_1. The direction of these electron transfers with respect to the membrane is unknown; it could range from essentially perpendicular to nearly parallel [see Robertson and Dutton (1988)].

(ii) Electron Transfer from SQ ($Q^{\bullet-}$) in the Q_{ow} Domain to cyt b_L. If histidines bridge the cyt b_L heme and the Q_{ow} domain ubiquinone as proposed in Figure 10, then the edge-to-edge distance will be approximately 4.9 Å. In a relatively nonpolar protein interior such as may prevail here, λ may be expected to be close to the 700 meV value found in analogous ubiquinone binding sites (Gunner & Dutton, 1989; Moser et al., 1992). With a ΔG° of approximately −120 meV as suggested in Figure 12, the nonadiabatic electron transfer rate should be around 1.7×10^{10} s^{-1} (60 ps).

(iii) Electron Transfer from Cyt b_L to Cyt b_H. The cyt b_L to cyt b_H electron transfer is likely also to be well described by nonadiabiatic electron-transfer theory. Recent modeling of the inter-heme distance (Farid, Robertson, and Dutton, manuscript in preparation) gives an edge-to-edge distance between 13 and 16 Å, depending on the orientations of the relevant α-helices and hemes. At the shortest distance between the cyt b_L and cyt b_H, together with the measured ΔG° of −150 meV and a reorganization energy of about 700 meV, a rate between 8×10^5 s^{-1} and 1.5×10^4 s^{-1} may be calculated. This range is consistent with estimation of greater than 10^4 s^{-1} by Crofts and Wang (1989).

(iv) Unproductive Electron Transfer from Cyt b_L to the [2Fe-2S] Cluster or Cyt c_1. Physiologically useful energy conversion in the cyt bc_1 complex requires electron transfer from ferro-cyt b_L to ferri-cyt b_H to be competitive with unproductive electron transfer from ferri-cyt b_L to a reoxidized [2Fe-2S] cluster or cyt c_1. A model in which a single ubiquinone molecule in the Q_o site spans the histidines that ligate the [2Fe-2S] cluster and cyt b_L heme will have a [2Fe-2S] cluster to cyt b_L edge-to-edge distance no greater than about 15 Å, close to the separation between the hemes of cyt b_L and cyt b_H. With a larger driving force of −380 meV between cyt b_L and the [2Fe-2S] cluster, an electron-transfer rate of at least 10^5 s^{-1} is expected even if the reorganization energy for this reaction rises to 1000 meV. Similarly, models such as those shown in Figure 10A,B in which two ubiquinones span the histidines, but with ring planes overlapping each other, are expected to have roughly comparable distances and electron-transfer rates. These unproductive rates are close enough to the rate of productive electron transfer from cyt b_L to cyt b_H that a charge separation yield failure of 5−90% seems possible, especially under *in vivo* conditions in which a transmembrane electric field would decrease the driving force and hence the rate of heme b_L to b_H electron transfer. In contrast, the model shown in Figure 13 in which the pair of ubiquinones in the Q_o site is arranged linearly in the most extended configuration between the [2Fe-2S] cluster and the cyt b_L heme gives a cyt b_L to the [2Fe-2S] cluster separation of up to 21 Å and an unproductive electron transfer rate about 30 s^{-1}, much slower than the productive cyt b_L to cyt b_H electron transfer. Depending on the values of the reorganization energy, the [2Fe-2S] cluster/cyt b_L edge-to-edge separation could indeed be as small as 17∼18 Å and still permit >99% quantum efficiency of charge separation from the cyt b_L to cyt b_H, even when the [2Fe-2S] cluster is reoxidized at a rate of 10^5 s^{-1}. Thus, a less extended arrangement shown in Figure 13 may be permissible, perhaps more like that indicated in Figure 10C,D. Similarly the distance between cyt b_L and cyt c_1 must be larger than 17−18 Å; indeed, using the distances described, a nearly linear arrangement of cyt b_L, [2Fe-2S] cluster and cyt c_1 would yield a separation of about 30 Å, assuring very stable charge separation.

REFERENCES

Aqvist, J., Fothergill, M., & Warshel, A. (1993) *J. Am. Chem. Soc. 115*, 631−635.

Atta-Asafo-Adjei, E., & Daldal, F. (1991) *Proc. Natl. Acad. Sci. U.S.A. 88*, 492−496.

Brandt, U., & Trumpower, B. (1994) *Crit. Rev. Biochem. Mol. Biol. 29*, 165−197.

Cha, Y., Murray, C. J., & Klinman, J. P. (1989) *Science 244*, 1030.

Clark, W. M. (1960) in *Oxidation−Reduction Potentials of Organic Systems*, Bailliere, Tindall and Cox, London.

Cramer, W. A., & Knaff, D. B. (1989) in *Energy Transduction in Biological Membranes*, Springer-Verlag, New York.

Crofts, A. R., & Wraight, C. A. (1983) *Biochim. Biophys. Acta 726*, 149−185.

Crofts, A. R., & Wang, Z. (1989) *Photosynth. Res. 22*, 69−87.

Crofts, A. R., Hacker, B., Barquera, B., Yun, C. H., & Gennis, R. (1992) *Biochim. Biophys. Acta 1101*, 162−165.

Daldal, F., Tokito, M. K., Davidson, E., & Faham, M. (1989) *EMBO J. 8*, 3951−3961.

Davidson, E., Ohnishi, T., Atta-Asafo-Adjei, E., & Daldal, F. (1992) *Biochemistry 31*, 3342−3351.

Degli Esposti, M., de Vries, S., Crimi, M., Ghelli, A., Patarnello, T., & Meyer, A. (1993) *Biochim. Biophys. Acta 1143*, 243−271.

de Vries, S. (1986) *J. Bioenerg. Biomembr. 18*, 195−224.

de Vries, S., Albracht, S. P. J., Berden, J. A., & Slater, E. C. (1981) *J. Biol. Chem. 256*, 11996−11998.

de Vries, S., Albracht, S. P. J., Berden, J. A., & Slater, E. C. (1982) *Biochim. Biophys. Acta 681*, 41−53.

Ding, H., Robertson, D. E., Daldal, F., & Dutton, P. L. (1992) *Biochemistry 31*, 3144−3158.

Ding, H., Daldal, F., & Dutton, P. L. (1995) *Biochemistry 34*, 15997−16003.

di Rago, J.-P., Coppee, J.-Y., & Colson, A.-M. (1989) *J. Biol. Chem. 264*, 14543−14548.

Dutton, P. L. (1978) *Methods Enzymol. 54*, 411−435.

Dutton, P. L. (1986) in *Encyclopedia of Plant Physiology* (Staehelin, A., & Arntzen, C. J., Eds.) Vol. 19, pp 197−237, Springer-Verlag, West Berlin.

Dutton P. L., & Jackson, J. B. (1972) *Eur. J. Biochem. 30*, 495−510.

Dutton, P. L., Wilson, D. F., & Lee, C. P. (1970) *Biochemistry 9*, 5077−5082.

Dutton, P. L., Petty, K. M., Bonner, H. S., & Morse, S. D. (1975) *Biochim. Biophys. Acta 387*, 536−556.

Ermler, U., Michel, H., & Schiffer, M. (1994) *J. Bioenerg. Biomembr. 26*, 5−15.

Foster, R., & Foreman, M. I. (1974) in *The Chemistry of the Quinonoid Compounds* (Patai, S., Eds.) Vol. 2, pp 257−334, John Wiley & Sons, London, New York, Sydney, and Toronto.
Gennis, R. B., Barquera, B., Hacker, B., van Doren, S. R., Arnaud, S., Crofts, A. R., Davidson, E., Gray, K., & Daldal, F. (1993) *J. Bioenerg. Biomembr. 25*, 195−209.
Giangiacomo, K. G., & Dutton, P. L. (1989) *Proc. Natl. Acad. Sci. U.S.A. 86*, 2658−2662.
Gray, K., & Daldal, F. (1995) in *Anoxygenic Photosynthetic Bacteria.* (Blankenship, Madigan, & Bauer, Eds.), pp 725−745, Kluwer Academic Publishers, Dordrecht, The Netherlands.
Gunner, M. R., & Dutton, P. L. (1989) *J. Am. Chem. Soc. 111*, 3400−3412.
Gunner, M. R., Braun, B. S., Bruce, J. M., & Dutton, P. L. (1985) in *Antennas and Pigments of Photosynthetic Bacteria* (Michel-Beyerle, M. E., Ed.) pp 298−305, Springer-Verlag, New York.
Gurbiel, R. J., Ohnishi, T., Robertson, D. E., Daldal, F., & Hoffman, B. M. (1991) *Biochemistry 30*, 11579−11584.
Jackson, J. B. (1988) in *Bacterial Energy Transduction* (Anthony, C., Ed.) pp 317−376, Academia Press, London.
Keske, J. M., Bruce, J. M., & Dutton, P. L. (1990) *Z. Naturforsh. C: Biosci. 45*, 430−435.
Kim, C. H., & Zitomer, R. S. (1990) *FEBS Lett. 266*, 78−82.
Kröger, A., & Klingenberg, M. (1973) *Eur. J. Biochem 34*, 358−368.
Leonard, K., Wingfield, P., Arad, T., & Weiss, H. (1981) *J. Mol. Biol. 149*, 259−274.
Link, T. A., Hagen, W. R., Pierik, A. J., Assmann, C., & von Jagow, G. (1992) *Eur. J. Biochem. 208*, 685−691.
Matsuura, K., Packham, N. Y., Mueller, P., & Dutton, P. L. (1981) *FEBS Lett. 131*, 17−22.
Matsuura, K., Bowyer, J. R., Ohnishi, T., & Dutton, P. L. (1983) *J. Biol. Chem. 258*, 1571−1579.
McComb, J. C., Stein, R. R., & Wraight, C. A. (1990) *Biochim. Biophys. Acta 1015*, 156−171.
Meinhardt, S. W., & Crofts, A. R. (1983) *Biochim. Biophys. Acta 723*, 219−230.
Mitchell, P. (1975) *FEBS Lett. 59*, 137−139.
Moser, C. C., & Dutton, P. L. (1992) *Biochim. Biophys. Acta 1101*, 171−176.
Moser, C. C., Keske, J. M., Warncke, K., Farid, R., S., & Dutton, P. L. (1992) *Nature 355*, 796−802.
Ohnishi, T., Brandt, U., & von Jagow, G. (1988) *Eur. J. Biochem. 176*, 385−389.
Ohnishi, T., Meinhardt, S. W., von Jagow, G., Yagi, T., & Hatefi, Y. (1994) *FEBS Lett. 353*, 103−107.
Packham, N. K., Berriman, J. A., & Jackson, J. B. (1978) *FEBS Lett. 89*, 205−210.
Petty, K. M., & Dutton, P. L. (1976) *Arch. Biochem. Biophys. 172*, 335−345.
Petty, K., Jackson, J., & Dutton, P. L. (1979) *Biochim. Biophys. Acta 546*, 17−42.
Prince, R. C. (1990) in *The Bacteria*, Vol. XII, pp 111−149, Academic Press, New York and London.
Prince, R. C., & Dutton, P. L. (1976) *FEBS Lett. 65*, 117−119.
Prince, R. C., & Dutton, P. L. (1977) *Biochim. Biophys. Acta 459*, 573−577.
Prince, R. C., Lindsay, J. G., & Dutton, P. L. (1975) *FEBS Lett. 51*, 108−111.
Robertson, D. E., & Dutton, P. L. (1988) *Biochim. Biophys. Acta 935*, 273−291.
Robertson, D. E., Prince, R. C., Bowyer, J. R., Matsuura, K., Dutton, P. L., & Ohnishi, T. (1984) *J. Biol. Chem. 259*, 1758−1763.
Robertson, D. E., Davidson, E., Prince, R. C, van den Berg, W. H., Marrs, B. L., & Dutton, P. L. (1986) *J. Biol. Chem. 261*, 584−591.
Robertson, D. E., Daldal, F., & Dutton, P. L. (1990) *Biochemistry 29*, 11249−11260.
Robertson, D. E., Ding, H., Chelminski, P. R., Slaughter, C., Hsu, J., Moomaw, C., Tokito, M., Daldal, F., & Dutton, P. L. (1993) *Biochemistry 32*, 1310−1317.
Siedow, J. N., Power, S., dela Rosa, F. F., & Palmer, G. (1978) *J. Biol. Chem. 253*, 2392−2399.
Takamiya, K.-I., & Dutton, P. L. (1979) *Biochim. Biophys. Acta 546*, 1−16.
Tokito, M. K., & Daldal, F. (1993) *Mol. Microbiol. 9*, 965−978.
Trumpower, B. L. (1990) *J. Biol. Chem. 265*, 11409−11412.
Tsai, A. L., Kauten, J. R., & Palmer, G. (1985) *Biochim. Biophys. Acta 806*, 418−426.
van den Berg, W. H., Prince, R. C., Bashford C. L., Takamiya, K., Bonner, W. D., & Dutton, P. L. (1979) *J. Biol. Chem. 254*, 8594−8604.
van Doren, S. R., Gennis, R. B., Barquera, B., & Crofts, A. R. (1993) *Biochemistry 32*, 8083−8091.
von Jagow, G., & Ohnishi, T. (1985) *FEBS Lett. 185*, 311−315.
Warncke, K., & Dutton, P. L. (1993a) *Proc. Natl. Acad. Sci. U.S.A. 90*, 2920−2924.
Warncke, K., & Dutton, P. L. (1993b) *Biochemistry 32*, 4769−4779.
Warncke, K., Gunner, M. R., Braun, B. S., Gu, L., Yu, C. A., Bruce, J. M., & Dutton, P. L. (1994) *Biochemistry 33*, 7830−7841.
Wikström, M. K. F., & Berden, J. A. (1972) *Biochim. Biophys. Acta 283*, 403−420.
Wraight, C. A. (1979) *Biochim. Biophys. Acta 548*, 309−327.
Yun, C. H., Wang, Z., Crofts, A. R., & Gennis, R. B. (1992) *J. Biol. Chem.* 267, 5901−5909.
Zannoni, D., & Marrs, B. (1981) *Biochim. Biophys. Acta 637*, 96−106.

BI950801S